

Applications and functions of rare-earth ions in perovskite solar cells

Limin Cang(苍利民), Zongyao Qian(钱宗耀), Jinpei Wang(王金培), Libao Chen(陈利豹), Zhigang Wan(万志刚), Ke Yang(杨柯), Hui Zhang(张辉), and Yonghua Chen(陈永华)

Citation: Chin. Phys. B, 2022, 31 (**3**): 038402. DOI: 10.1088/1674-1056/ac373a

Journal homepage: http://cpb.iphy.ac.cn; http://iopscience.iop.org/cpb

What follows is a list of articles you may be interested in

Theoretical investigation of halide perovskites for solar cell and optoelectronic applications

Jingxiu Yang(杨竞秀), Peng Zhang(张鹏), Jianping Wang(王建平), and Su-Huai Wei(魏苏淮)†

Chin. Phys. B, 2020, 29 (**10**): 108401. DOI: 10.1088/1674-1056/abb3f6

SiO_2 nanoparticle-regulated crystallization of lead halide perovskite and improved efficiency of carbon-electrode-based low-temperature planar perovskite solar cells

Zerong Liang(梁泽荣), Bingchu Yang(杨兵初), Anyi Mei(梅安意), Siyuan Lin(林思远), Hongwei Han(韩宏伟), Yongbo Yuan(袁永波), Haipeng Xie(谢海鹏), Yongli Gao(高永立), Conghua Zhou(周聪华)

Chin. Phys. B, 2020, 29 (**7**): 078401. DOI: 10.1088/1674-1056/ab8da5

Factors influencing the performance of paintable carbon-based perovskite solar cells fabricated in ambient air

Wei-Kang Xu(许伟康), Feng-Xiang Chen(陈凤翔), Gong-Hui Cao(曹功辉), Jia-Qi Wang(王嘉绮), Li-Sheng Wang(汪礼胜)

Chin. Phys. B, 2018, 27 (**3**): 038402. DOI: 10.1088/1674-1056/27/3/038402

Importance of ligands on TiO_2 nanocrystals for perovskite solar cells

Yao Zhao(赵耀), Yi-Cheng Zhao(赵怡程), Wen-Ke Zhou(周文可), Rui Fu(伏睿), Qi Li(李琪), Da-Peng Yu(俞大鹏), Qing Zhao(赵清)

Chin. Phys. B, 2018, 27 (**1**): 018401. DOI: 10.1088/1674-1056/27/1/018401

Improving power conversion efficiency of perovskite solar cells by cooperative LSPR of gold-silver dual nanoparticles

Peng Liu(刘鹏), Bing-chu Yang(杨兵初), Gang Liu(刘钢), Run-sheng Wu(吴闰生), Chu-jun Zhang(张楚俊), Fang Wan(万方), Shui-gen Li(李水根), Jun-liang Yang(阳军亮), Yong-li Gao(高永立), Cong-hua Zhou(周聪华)

Chin. Phys. B, 2017, 26 (**5**): 058401. DOI: 10.1088/1674-1056/26/5/058401

TOPICAL REVIEW — Emerging photovoltaic materials and devices

Applications and functions of rare-earth ions in perovskite solar cells

Limin Cang(苍利民)[1], Zongyao Qian(钱宗耀)[2], Jinpei Wang(王金培)[2], Libao Chen(陈利豹)[2], Zhigang Wan(万志刚)[1], Ke Yang(杨柯)[1], Hui Zhang(张辉)[2,†], and Yonghua Chen(陈永华)[2,‡]

[1] *Research Center, Ancai Hi-Tech Co., Ltd., Anyang* 455000, *China*

[2] *Key Laboratory of Flexible Electronics, Institute of Advanced Materials, Nanjing Tech University, Nanjing* 211800, *China*

(Received 29 August 2021; revised manuscript received 19 October 2021; accepted manuscript online 6 November 2021)

The emerging perovskite solar cells have been recognized as one of the most promising new-generation photovoltaic technologies owing to their potential of high efficiency and low production cost. However, the current perovskite solar cells suffer from some obstacles such as non-radiative charge recombination, mismatched absorption, light induced degradation for the further improvement of the power conversion efficiency and operational stability towards practical application. The rare-earth elements have been recently employed to effectively overcome these drawbacks according to their unique photophysical properties. Herein, the recent progress of the application of rare-earth ions and their functions in perovskite solar cells were systematically reviewed. As it was revealed that the rare-earth ions can be coupled with both charge transport metal oxides and photosensitive perovskites to regulate the thin film formation, and the rare-earth ions are embedded either substitutionally into the crystal lattices to adjust the optoelectronic properties and phase structure, or interstitially at grain boundaries and surface for effective defect passivation. In addition, the reversible oxidation and reduction potential of rare-earth ions can prevent the reduction and oxidation of the targeted materials. Moreover, owing to the presence of numerous energetic transition orbits, the rare-earth elements can convert low-energy infrared photons or high-energy ultraviolet photons into perovskite responsive visible light, to extend spectral response range and avoid high-energy light damage. Therefore, the incorporation of rare-earth elements into the perovskite solar cells have demonstrated promising potentials to simultaneously boost the device efficiency and stability.

Keywords: perovskite, solar cells, rare-earth ions, power conversion efficiency

PACS: 84.60.Jt, 88.40.hj, 71.20.Eh, 88.40.H− **DOI:** 10.1088/1674-1056/ac373a

1. Introduction

Solar cells, which can directly convert the most abundant and inexhaustible solar energy into electricity, offer a valuable solution to energy shortage and environmental pollution in the future life. However, the large-area applications of the traditional crystalline silicon and thin film solar cells are restricted because of the high production cost and long payback period. The new generation solar cells including dye-sensitized, organic and perovskites solar cells have attracted increasingly attention owing to their promising advantages of ease of fabrication, light weight and cost-effective manufacturing. Among them, the perovskite solar cells have been recognized as one of the most ideal substitutes for the silicon solar cells because of their high efficiency and low production cost.[1–5] However, state-of-the-art perovskite solar cells suffer from some challenges, such as trap assisted non-radiative recombination, mismatched light absorption with solar spectrum, performance degradation under solar illumination, and so on, leading to unintentional energy loss, limited photogenerated current, and short operational durability,[6,7] respectively. The recent investigations have revealed that the incorporation of rare-earth elements in the perovskite solar cells is able to mitigate these issues owing to their unique optical and electrical properties, and some significant progress have been achieved. In this review, we firstly introduced some fundamental information about the perovskite solar cells and photophysical properties of the rare earth elements. Secondly, the recent progress of the application of rare-earth ions in perovskite solar cells, including their specific functions and the in-depth work mechanism were systematically reviewed. In the end, we provided an outlook on what the future efforts should be focused on the development of rare-earth related materials for the performance improvement of perovskite solar cells.

2. Perovskite solar cells

2.1. Introduction of perovskite solar cells

Lead halide perovskites are a type of semiconductors with cubic crystal structure of ABX_3 (Fig. 1), where A is a monovalent cation in terms of methylammonium (MA^+), formamidinium (FA^+) and Cs^+, B is a divalent metal ion of Pb^{2+} or Sn^{2+}, and X is a monovalent anion of I^-, Br^- or Cl^-. The perovskites present some promising optoelectronic properties, such as high light absorption ability, tunable bandgap,

†Corresponding author. E-mail: iamhuizhang@njtech.edu.cn
‡Corresponding author. E-mail: iamyhchen@njtech.edu.cn

© 2022 Chinese Physical Society and IOP Publishing Ltd

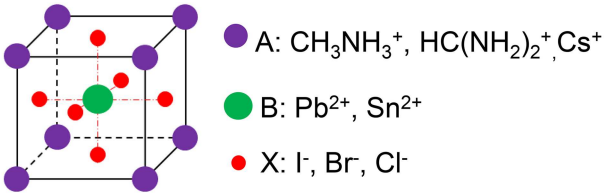


Fig. 1. Crystal structure of ABX_3 perovskite.

ambipolar charge transport, long electron/hole diffusion lengths, cost-effective solution processability and high charge mobility.[8] The perovskite solar cells were derived from dye-sensitized solar cells, which was initially developed by Grätzel *et al.*[9] In 2009, Kojima *et al.*[1] firstly replaced the light absorbing organic dyes with the perovskites of $MAPbBr_3$ and $MAPbI_3$ in the dye-sensitized solar cells, resulting in the first solar cells based on perovskites with power conversion efficiency of 3.8%. However, the perovskites are easily corroded by the liquid electrolytes in the perovskite-sensitized solar cells, leading to extremely poor stability. Until 2012, Kim *et al.* used the solid state hole transport material of spiro-OMeTAD to replace the liquid electrolytes, resulting in the so-called perovskite solar cells with simultaneously improved efficiency and stability.[10] Since then, the perovskite solar cells have obtained aggressive research attention with yearly thousands of publications, and the highest certified efficiency has recently reach up to 25.5%,[11] not far from the efficiency of crystalline silicon solar cells.

2.2. Device architecture

In a typical perovskite solar cell, the photosensitive perovskite layer is sandwiched between a transparent front electrode and a reflective back electrode. In general, charge transport layers such as electron transport layer (ETL) and hole transport layer (HTL) are inserted between the cathode/perovskite or perovskite/anode interfaces, respectively, to facilitate the majority charge collection at the respective electrode. In some cases, a mesoporous layer is inserted as a scaffold layer to enlarge the contract area between the perovskite and charge transport layer. According to the layer sequence and morphology structure of the charge transport layer, the perovskite solar cells can be classified into four types such as regular mesoporous structure, regular planar structure, inverted mesoporous structure and inverted planar structure as demonstrated in Fig. 2.

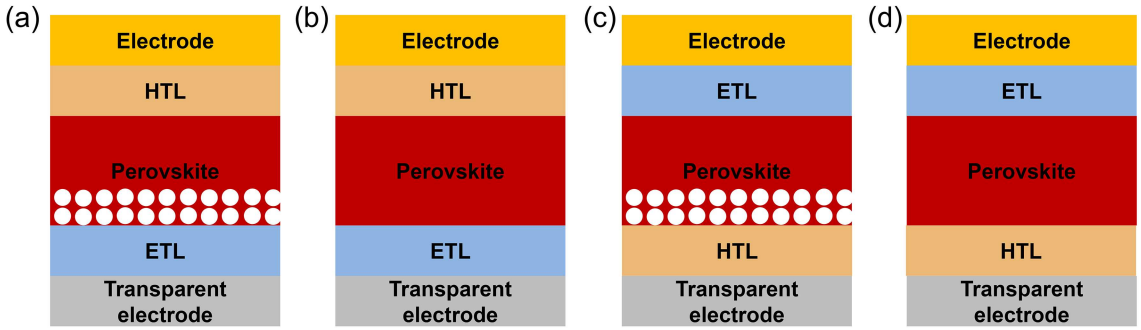


Fig. 2. Device architectures of perovskite solar cells: (a) regular mesoporous structure; (b) regular planar structure; (c) inverted mesoporous structure; (d) inverted planar structure.

2.3. Operational mechanism

Under sunlight illumination, the photons with energy over the bandgap of the perovskite can be captured, and the electrons can be excited from the ground state to the conduction band, leaving the positively charged holes retained at the valence band orbits. Owing to the small binding energy, the electrons can overcome the attractive force of the holes and transport to the cathode with the favor of ETL. In the meanwhile, the holes can transport across the HTL and be collected at the anode. The specific energy band structure diagram and charge transport dynamic of the perovskite solar cells are clearly demonstrated in Fig. 3.

2.4. Present challenges of perovskite solar cells

The golden triangle of photovoltaic technologies contains production cost, power conversion efficiency and long-term stability, as shown in Fig. 4. Even though the solar cells based on perovskites have achieved rapid progress in the last decade, the pursuit of highly reproducible, efficient and operationally stable perovskite solar cells is still the main target for their further development towards practical applications. The recent researches have been mainly focused on the development of strategies to fabricate high quality perovskite thin films, synthesis high mobility and energy level matched charge transport materials, design environmentally friendly manufacturing methods,[8] construct optical architectures to maximize light absorption.[12–15] However, the perovskite materials are vulnerable to various aging stresses such as oxygen, moisture and ultraviolet (UV) light, seriously restricted their long term stability.[16–19] The penetration of oxygen and moisture into the perovskite layer can be effectively prevented by introducing extra encapsulating layers,[20,21] while the UV light illumination is inevitablev for all photovoltaic devices, which is prone to decompose the perovskite materials and cause the de-

vice performance degradation. Therefore, strategies to efficiently block the UV light are highly demanded to protect the device from the high energy light damage.

Moreover, it was realized that some unintentional defect states are prone to be generated during the perovskite growth, which can act as charge recombination centers to cause unnecessary energy loss and accelerate performance degradation. And also, energetic barriers due to the mismatched energy level between the perovskite and charge transport layers can induce charge accumulation at the interface and prohibit the charge transport and extraction. Even though the perovskites exhibited high tolerance on the defect states, the presence of the defect states and high density charge accumulation can cause limited power conversion efficiency, seriously hysteresis and performance degradation.

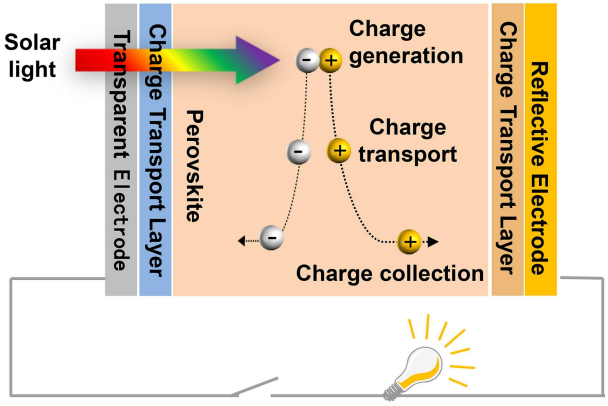


Fig. 3. Operational principle of perovskite solar cells, including charge generation, charge transport and charge collection at respective electrodes.

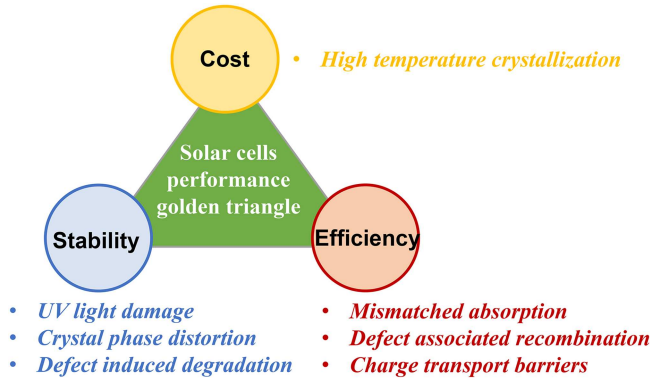


Fig. 4. Golden triangle of solar cells performance including the current challenges those need to be addressed.

In addition, the solar spectrum of AM1.5G is composed of ultraviolet (UV) light, visible light and infrared light ranging from 280 nm to 2500 nm. To improve the power conversion efficiency of solar cells, the light harvesting should be maximized in order to take advantages of the full solar spectrum. However, the perovskites can only absorb photons with energy higher than their bandgaps, most of the photons at near infrared (NIR) wavelength region cannot be captured.[22] Even though the bandgap is tunable by varying the chemical composition of the perovskites, but the most efficient perovskite solar cells can only absorb a small portion of solar spectrum in the ultraviolet and visible light ranges.[23] In particular, state-of-the-art efficient perovskite solar cells usually employ perovskites in terms of $CH_3NH_3PbI_3$ ($MAPbI_3$), $CH(NH_2)_2PbI_3$ ($FAPbI_3$) or their mixtures as the photoactive layers.[8] The absorption of these perovskites can cover the entire visible light spectrum range with a cutoff at $\sim$ 850 nm, which is recognized as one of the best light absorbing materials. Even though the solar energy in the NIR region occupies more than half of the total solar energy, it cannot be captured by the perovskites. Therefore, the energy loss in NIR light resulted in limited efficiency of perovskite solar cells.[24]

Therefore, in order to achieve high performance perovskite solar cells, the aforementioned issues such as the high-energy light induced performance degradation, non-radiative recombination and mismatch between the perovskite absorption and solar spectrum are the remaining challenges that need to be urgently addressed.

3. Rare-earth ions

Rare-earth elements, also called lanthanides or inner transition metals, are consisted of 15 lanthanides from lanthanum to lutetium[25] and two elements of scandium and yttrium in group III B.[26,27] The physical and chemical properties of the rare-earth elements are quite similar, and their electronic configuration can be present in a common formula of $4f^{0,2\,\text{to}\,14}5d^{0,1}6s^2$. Owing to the presence of abundant 4f orbits and some vacant 5d orbits, different intermediate energy states can be generated in the rare-earth containing materials, rendering them unique photophysical properties. Therefore, the electronic properties of some materials, such as metal oxides, perovskites, etc., can be adjusted by properly doping different types of rare-earth ions. Moreover, the rare-earth ions are usually found in the 3+ or 2+ oxidation state, which can strongly associate with negatively charged ions, and coupling the rare-earth ions with other crystalline materials can modify the crystallization dynamics and reduce intra-gap trap states. And also, the elements in the crystal lattice can be substituted by rare-earth elements with suitable ionic radius, thus affecting the unit cell parameters and phase stability of the target crystals.

More importantly, the rare-earth containing materials generally exhibit two different luminescence pathways, such as f–f transition and f–d transition, which makes them ideal phosphors with light emission ranging from UV to NIR region and the potential to absorb low energy photons.[27,28] The f–f transition allows a narrow peak, weak intensity and relatively less-efficient luminescence, while the photoluminescence based on the f–d transition exhibits broadband, strong intensity and high luminescence efficiency. The up-conversion

(UC) and down-conversion (DC) properties of rare-earth ion-doped materials endow them promising application potentials in optoelectronic devices. Particularly, up-conversion is a nonlinear optical phenomenon that converts multiple low-energy photons into high-energy photons, which is an anti-Stokes process. In a typical up-conversion system as demonstrated in Fig. 5(a), the rare-earth ions can absorb the low-energy photons under NIR light excitation via either excited state absorption or energy transfer between two ions or cross-relaxation energy transfer and the energy can then be transferred to the neighboring Er^{3+} and Tm^{3+} ions for up-conversion emission. The luminescent light is in the wavelength range of 400–700 nm, which is within the perovskite responsive wavelength range. The general energy diagram of the up-converting is illustrated in Fig. 5(b). Down-conversion (DC) is a linear optical phenomenon, which converts one high-energy photon into multiple low-energy photons. Figures 5(c) and 5(d) illustrate the schematic diagram and principle down-conversion process based on a single rare earth ion of I or two rare-earth ions of I and II, where the I is a sensitizer ion with wide bandgap which can absorb high energy photons, the II is an activator ion, which can accept the energy from I. Owing to these unique luminescent properties, the incorporation of rare-earth can open many application windows in terms of medical imaging devices, automobile catalysts, phosphors in color television and optoelectronic devices.[29–33]

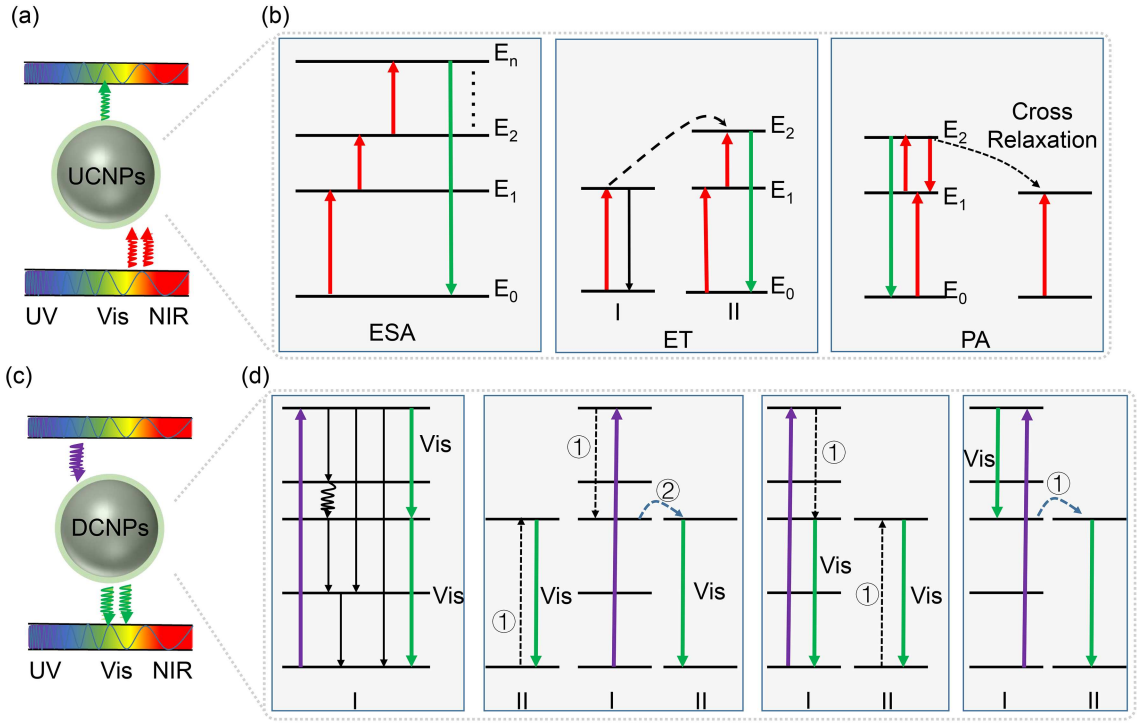


Fig. 5. (a) The schematic diagram and (b) principle up-conversion processes in rare-earth ions doped nanoparticles under near-infrared light excitation, in which the ESA, ET and PA represent excited state absorption, energy transfer and photon avalanche, respectively. (c) The schematic diagram of and (d) principle down-conversion luminescence: UV light absorption and down conversion by emission of two visible photons on a single ion or two ions, in which ① is the relaxation and ② is the energy transfer between the two ions.

4. Application of rare-earth ions in perovskite solar cells

As aforementioned, the rare-earth ions can be coupled with both the charge transport metal oxides and the photoactive perovskites in the multilayered perovskite solar cells, and their functions can be summarized in Fig. 6.[34–36] In particular, the incorporation of rare-earth ions into the metal oxides or perovskites has a major effect on their charge carrier mobility, band structures and absorption/luminescence properties owing to the various energy-level transition orbits of the rare-earth ions, resulting in modified charge transport dynamics and well-aligned energy level in the corresponding perovskite solar cells. Moreover, the added rare-earth ions can adjust the perovskite crystallization via the strong interaction between the rare-earth ions and the halides in the perovskite precursor, facilitating the perovskite growth with reduced formation barriers and adjustable thin film morphology. Furthermore, the incorporation of rare-earth ions can stabilize the crystal phase structure with enhanced binding energy of the crystal units, tailored crystal size and dimensions, eliminated defect states. From the other aspect, the application of rare-earth elements in perovskite solar cells can not only enhance the light harvesting with extended spectra response owing to their up-converting, down-converting or light scattering properties,[37] but also avoid light induced performance degradation by converting the high energy light into visible light regions to boost the device stability.

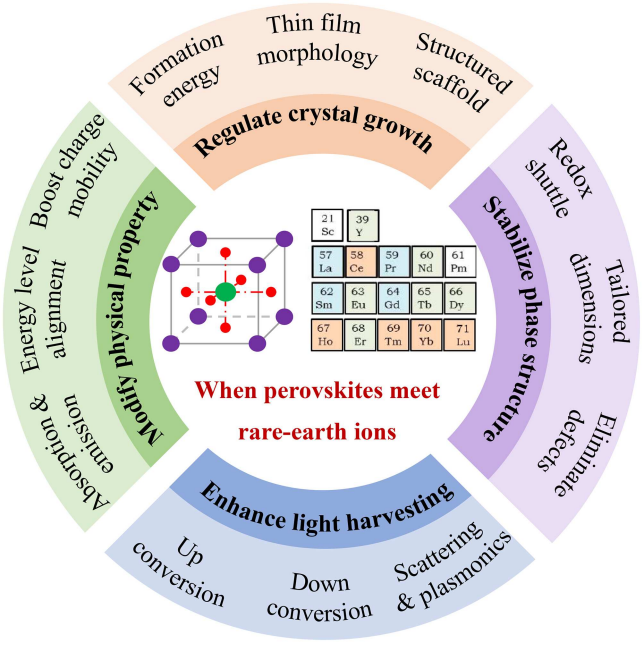


Fig. 6. Summary of functions of rare-earth ions in perovskite solar cells.

4.1. Optimizing charge transport layers

Metal oxide semiconductors in terms of TiO_2, SnO_2, NiO_x are the most frequently employed ETLs, HTLs or scaffolds in perovskite solar cells. However, the metal oxides suffer from high density of defect states and difficulty to adjust their electronic properties. Among the metal oxides, TiO_2 and SnO_2 are the most frequently used ETLs in perovskite solar cells owing to the relatively high electron affinity and capabilities of electron transporting and holes blocking.[38,39] But the significant drawbacks of the metal oxides such as high density of electronic defects, environmental instability and mismatched energy level with perovskites lead to strong hysteresis, low efficiency and rapid degradation under ultraviolet illumination of the corresponding solar cells.[40] In particular, oxygen vacancies in the metal oxide layer are one of the main sources for the formation of defect states, for instance, the Ti (IV) in TiO_2 is prone to be reduced to Ti (III) (Fig. 7(a)), which can not only act as pathways for non-radiative charge recombination, but also induce fast performance decay upon continuous UV irradiation.[41] It has been revealed that introducing some rare-earth elements in the TiO_2 layer can effectively eliminate the defect states as demonstrated in Fig. 7(b). For examples, the incorporation of Nd^{3+} ions in TiO_2 layer can successfully enhance the efficiency and stability of the corresponding perovskite solar cells. Precisely, the added Nd^{3+} can partially substitute Ti^{4+} in the TiO_2 crystal lattice without obviously affecting the crystal structure as confirmed by the x-ray diffraction spectra (Fig. 7(c)), leading to reduced trap states and mitigated electron non-radiative recombination (Fig. 7(d)). Moreover, the trivalent dopants of the rare-earth elements in TiO_2 can effectively reduce the oxygen vacancies to prevent the high energy light induced desorption of O_2, which can significantly enhance their operational stability (Fig. 7(e)).[42]

Furthermore, the rare-earth ions can be used to modify the Fermi levels of the metal oxides. Owing to the high binding affinity of the rare-earth ions to oxygen, the doping of La,[43] Sm,[44] Eu,[45] Y[46,47] ions in the TiO_2 layer illustrated a shift of the quasi-Fermi level by eliminating oxygen atoms on the surface of TiO_2. The well-aligned Fermi level with the corresponding perovskites can reduce the energetic barriers for charge transport, thereby enhancing the open circuit voltage and power conversion efficiency (Fig. 7(f)). In addition, the electron mobility of the metal oxides was generally lower than the hole mobility of their counterpart such as spiro-OMeTAD, leading to unbalanced charge transport and serious hysteresis.

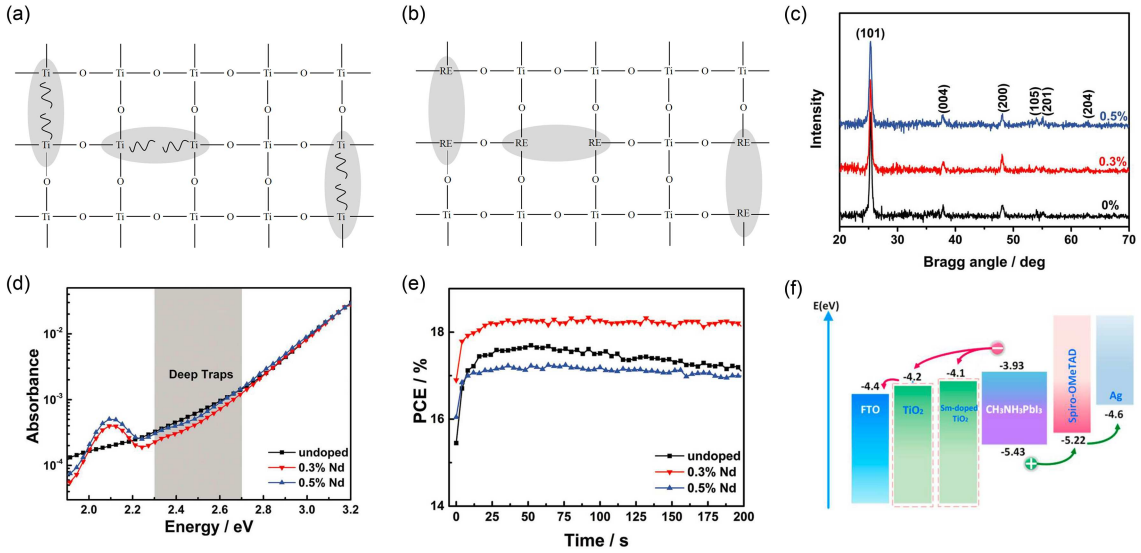


Fig. 7. (a) Oxygen vacancies in TiO_2 due to the formation of Ti(III) defects that form deep electronic traps and (b) substitution of rare-earth (RE) at the Ti(III) sites for defect passivation,[41] (c) XRD spectra, (d) photothermal deflection spectra and (e) stability of the device based on pristine TiO_2 and Nd-doped TiO_2,[42] respectively. (f) Schematic illustration of the energy levels in perovskite solar cells based on pristine and rare-earth ions doped TiO_2.[44]

The conductivity of the metal oxide layers can be enhanced by the doping of rare-earth ions due to the increased carrier density.[46,48] For examples, SnO_2 has recently emerged as an promising candidate of TiO_2 owing to the high electron mobility and well aligned energy level with perovskites.[39,49] Doping with n-type ions such as Y^{3+} can optimize the energy level alignment and increase the electron mobility of SnO_2,[50] which accelerates charge extraction and reduces non-radiative charge recombination, resulting in significantly enhanced short-circuit current (J_{SC}) and fill factor (FF).[51–53] Moreover, it was known that the electron mobility of metal oxides is related with the crystal structures, for examples, the electron mobility of anatase TiO_2 is higher than that of rutile phase,[54] and mixing the rutile phase and anatase phase TiO_2 can generate a built-in electric field in ETL layer to promote charge transport and eliminate charge recombination.[55] Ren and co-workers[56] employed a Er-doped TiO_2 as ETL in perovskite solar cells. As they found that it was difficult to replace Ti^{4+} with Er^{3+} in the crystal lattice because the ionic radius of Er^{3+} is much larger than that of Ti^{4+}. The formation of chemical bond of Er–O–Ti can only occur at high temperature thermal annealing, which is beneficial to restrain the phase transition from anatase to rutile and generate a mixed anatase and rutile phase of TiO_2.

The HTLs are considered to be a crucial layer to achieve high performance inverted perovskite solar cells, which exhibit less hysteresis with respect to regular configurations and are prone to be integrated with silicon solar cells for tandem devices. Compared to organic HTLs in terms of PEDOT:PSS, P3HT, PTAA and Spiro-OMeTAD, the nickel oxide (NiO_x) is one of the most promising inorganic HTLs for inverted perovskite solar cells due to its high chemical resistance, low production cost and superior light transmission.[57–59] However, the efficiency of perovskite solar cells based on NiO_x is still lower than that based on organic HTLs because of the low conductivity and difficulty in tuning the electronic property of NiO_x.[60,61] Many investigations have demonstrated that the electronic structure of the NiO_x layer can be effectively varied through additive engineering, thus improving the performance of inverted perovskite solar cells.[62,63] Many rare-earth ions such as Ce^{3+}, Nd^{3+}, Eu^{3+}, Tb^{3+}, Yb^{3+} [48] and La^{3+} [64] have been explored as additives in the preparation of the NiO_x layer. It was found that these rare-earth ions could hardly entered into the crystal lattice of NiO_x due to the big difference of the ionic radius between the rare-earth ions and Ni, and the dopants were mainly found at the interstitial site or the thin film surface to effectively eliminate the defect states.[65–67] In 2018, Hu and co-workers [68] firstly introduced yttrium ion (Y^{3+}) ions as dopants in the preparation of NiO_x HTL in inverted perovskite solar cells. It was found that Y^{3+} can be successfully incorporated into the crystal lattice of the NiO_x due to the small ionic radius of the Y^{3+}.[68] Because the Y^{3+} ions have an occupied 4d orbital, the electronic configurations and electrical conductivity of the NiO_x can be modified through Y^{3+} doping,[47,69,70] resulting in significant enhancement of photogenerated current compared to the device based on pristine NiO_x.[68]

4.2. Modifying the morphology of metal oxide thin films

It was known that the morphology of underneath charge transport layers determines the thin film quality of the upper perovskite layers and the interfacial contact between the CTL and the perovskite, and the rare-earth ions were found to be able to modify the thin film morphology of the metal oxide layers and align the nanostructure of the scaffold layers.[71,72] For examples, the SnO_2 thin films can be simply deposited via direct spin-coating of SnO_2 nanoparticles, while the spontaneous aggregation of SnO_2 nanoparticles can result in pinholes or island morphology in the as deposited films (Fig. 8(a)), seriously restricting the device performance. It was found that the addition of La^{3+} can mitigate the SnO_2 nanoparticle aggregation to prevent the formation of pinholes (Fig. 8(b)).[71] And also, the doping of some rare-earth ions such as Eu^{3+}, La^{3+} into NiO_x, can obviously reduce the crystal size of NiO_x crystals (Figs. 8(c) and 8(d)) due to the formation of rare-earth–O bonding that restricted the growth of large crystals, enabling the formation of compact and uniform NiO_x thin films.[64]

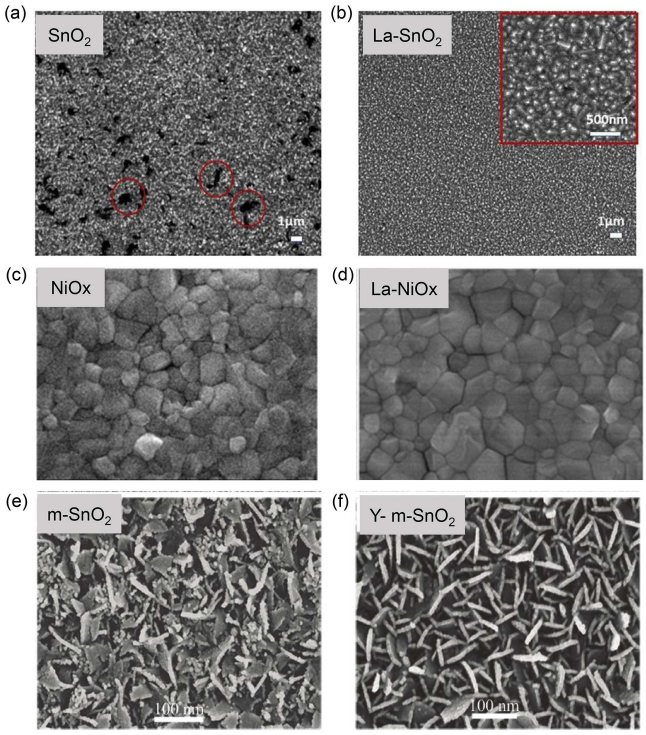


Fig. 8. Thin film morphologies of rare-earth ions doped metal oxides: planar (a) pristine SnO_2 and (b) La doped SnO_2,[69] (c) pristine NiO_x and (d) La doped NiO_x,[64] mesoporous (e) pristine SnO_2 and (f) Y doped SnO_2.[72]

In mesoporous structured perovskite solar cells, the scaffold layer plays an important role to improve the contact area

between the perovskite and CTL. However, the scaffold layer is composed of structured nanoparticles with numerous grain boundaries and morphological defects, leading to serious non-radiative charge recombination. Moreover, the pore-filling of perovskite into the randomly featured nanoparticles is the other difficulty. Therefore, strategies need to be developed to regulate the growth of the scaffold layer with reduced defect states and uniform and well-aligned nanostructures.[73] For examples, Guo and co-workers[74] have integrated Sc^{3+}, $Y^{3+}$and La^{3+} into the SnO_2 nanospheres. The doping of rare-earth ions can affect the growth dynamics and enable the formation of uniform, monodispersed SnO_2 with enlarged pore width and specific surface area, facilitating the perovskite infiltration. And also, the mesoporous SnO_2 with regular structure can improve perovskite coverage condition, allowing for the growth of uniform and compact perovskites with enlarged grain size. Yang and co-workers[72] synthesized yttrium-doped SnO_2 nanosheet arrays via low-temperature hydrothermal process. It was found that the hydrolysis of the incorporated Y^{3+} can modify the acidity of the precursor solution and hence promote the growth of uniform and homogeneously distributed Y-SnO_2. The well-aligned SnO_2 nanosheet array (Figs. 8(e) and 8(f)) can effectively improve perovskite infiltration. In the meanwhile, the Y^{3+} can be embedded into the crystal lattice of SnO_2 and optimize the energy level of SnO_2. Therefore, the increased contact area and reduced energetic barrier between the perovskite and SnO_2 can improved the efficiency with significantly reduced hysteresis.

4.3. Tuning optoelectronic property of perovskites

The optoelectronic property of the perovskites can be tailored by the doping of rare-earth ions. For examples, the B-site cations of the perovskite can be partially substituted by rare-earth ions such as Eu^{2+} because of the similar ionic radius (Eu^{2+}, 117 pm, Pb^{2+}, 119 pm). In 2019, Wu and co-workers[75] introduced EuI_2 as dopants into the $MAPbI_3$ perovskite. It was found that the incorporated Eu^{2+} can be embedded into the perovskite crystal lattice to form $MAPb_{1-x}Eu_xI_3$, which was consistent with some other reports.[76] The as formed $MAPb_{1-x}Eu_xI_3$ can substantially enhance the absorption at the UV-vis wavelength region due to the formation of some impurity energy levels by the EuI_2 doping. Furthermore, partial substitution of Eu^{2+} into the perovskite lattice affected the electronic orbits and improved the charge mobility, resulting in improved short circuit current density and the conversion efficiency, as calculated by Suzuki.[77] And also, the absorption edge (Fig. 9(a)) and the light emission (Fig. 9(b)) properties can be finely tailored by incorporating different rare-earth ions in the perovskites.[76] The reason for the variation of the optical property was ascribed to the different electronic orbitals and ionic radius of the rare-earth ions, which can generate intermediate energetic levels and induce lattice vibration in the doped perovskite crystals. Moreover, the rare-earth ions doping can enhance the photoluminescence property of the perovskites. For instance, the doping of Ce^{3+} into $CsPbBr_3$ perovskite nanocrystal can improve the lattice order and enrich the conduction band edge states, leading to significantly enhanced PL (Fig. 9(c)).[78] Furthermore, the as formed intermediate energetic states can boost the photoluminescence quantum efficiency above 100% of the rare-earth ions doped perovskites, in which the captured photon can be split into two low energy photons and emit along the dopants as illustrated in Fig. 9(d), to open many novel application windows.[79]

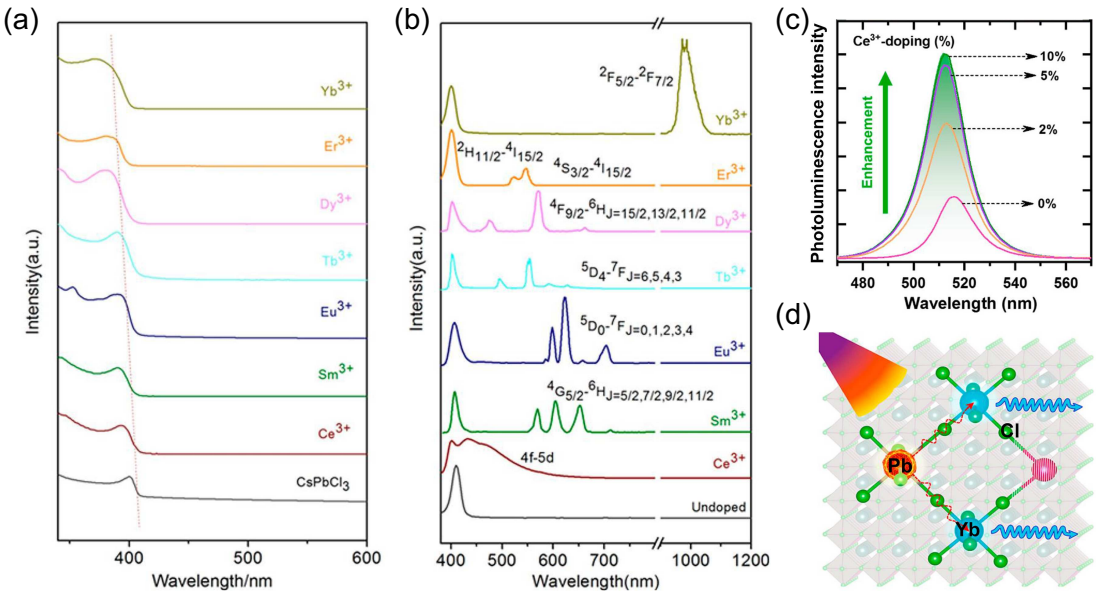


Fig. 9. Optical properties of the pristine $CsPbCl_3$ perovskite nanocrystals and doped with different lanthanide ions. (a) UV-vis absorption spectra and (b) photoluminescence spectra of the $CsPbBr_3$ doped with different rare-earth ions.[76] (c) Enhanced photoluminescence of $CsPbBr_3$ via the doping of Ce^{3+} at different concentrations.[78] (d) Schematic illustration of quantum cutting mechanism.[79]

4.4. Regulating perovskite crystallization

The thin film morphology of the perovskite layer is another determining factor on the efficiency of perovskite solar cells. The incorporation of rare-earth ions can affect the perovskite crystallization to modify the thin film morphology and lower the formation energy. For examples, when the Eu^{3+} ions were added into inorganic $CsPbI_2Br$ perovskite precursor,[80,81] as it was illustrated in Fig. 10(a) that the incorporated Eu^{3+} ions can strongly interact with negatively charged halide plumbates (PbX_3^-, PbX_4^{2-}, PbX_6^{4-}, X = I, Br) and create complex of $Eu-PbX_2$, which can be used as nucleus to facilitate the perovskite growth with uniformed surface coverage and homogeneously distributed grain size (Figs. 10(b) and 10(c)),[82] thereby resulting in improved device performance (Fig. 10(d)).[83] And also, Duan and co-workers[84] reported a work on the doping of different rare-earth ions (Sm^{3+}, Tb^{3+}, Ho^{3+}, Er^{3+}, and Yb^{3+}) into $CsPbBr_3$ perovskite. As they found that these ions can strongly associate with the halide ions and hence affect the perovskite crystallization, and it was interestingly found that the crystal size was strongly related with the atomic number of the rare-earth ions. Particularly, the grain size is gradually increased and the perovskite thin films become more compact with the decrease of atomic number of the rare-earth ions.

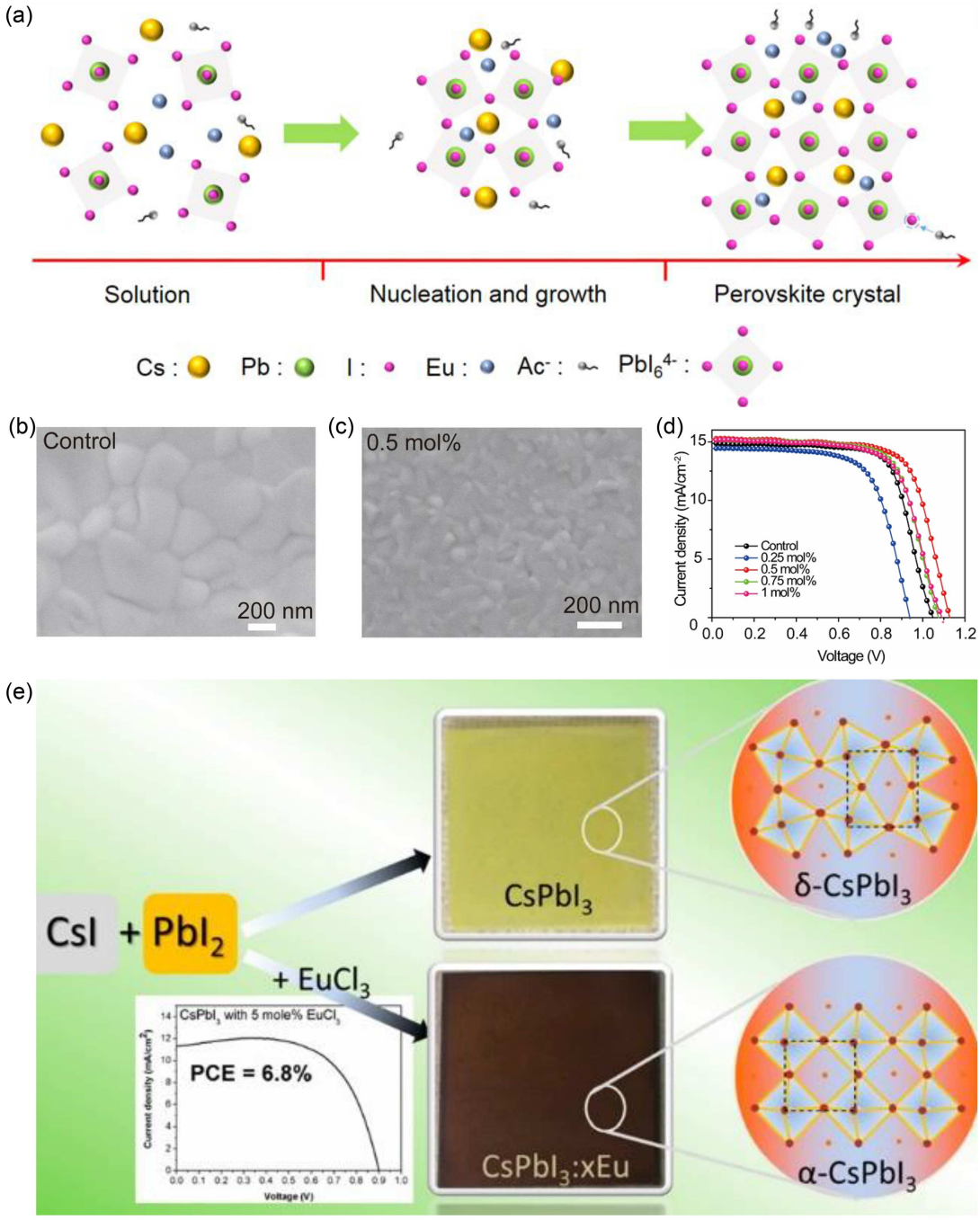


Fig. 10. Effect of the rare-earth ions on the perovskite crystallization. (a) Schematic illustration of $CsPbI_2Br$ perovskite crystallization with the doping of rare-earth of Eu^{3+}, thin film morphologies of the (b) pristine perovskite and (c) Eu doped perovskite, and (d) the performance of corresponding perovskite solar cells.[82] (e) Stabilization of $CsPbI_3$ at room temperature.[87]

It was known that the perovskites are usually formed at relatively high temperature, for instance, the $CsPbI_3$ usually presents a yellow non-perovskite phase at room temperature because the black perovskite phase is only stabilized at temperatures above 335 °C,[85] increasing the production cost. The interaction between the rare-earth ions and the perovskite precursor in the solution can lower the perovskite formation energy by modifying the one-step conversion from precursor to perovskite with larger formation energy barrier to the two-step conversion from precursor to complex and then to perovskite with reduced formation energy barrier, allowing the perovskite growth at low temperature.[86] In 2018, Jena and co-workers[87] tried to dope $EuCl_3$ into the $CsPbI_3$ perovskite, and it was found that the black perovskite phase of $CsPbI_3$ can be stabilized at room temperature and ambient condition. They attributed the low temperature phase stabilization to the reduced grain size and crystal structure distortion (Fig. 10(e)), but the underlying mechanism still needs further investigation.

4.5. Stabilizing perovskite phase structure

The doping of rare-earth ions can stabilize the perovskite crystal structure and boost the device stability. First of all, the element substitution in the crystal lattice or interstitial doping at grain boundaries by the rare-earth elements can effectively reduce the trap states, where the degradation is likely to occur, via strong interaction with antisite defects in the perovskite crystals, effectively stabilizing the crystal structure. For examples, the incorporated Eu^{3+} in $CsPbI_2Br$ perovskite were found at the interstices of the crystal lattice and at the grain boundaries of the perovskites, and the transition of the perovskite phase to non-perovskite phase can be significantly mitigated or can be partially repaired via thermal treatment after the Eu^{3+} doping, leading to improved thermal stability.[82] The incorporation of rare-earth ions in the perovskite lattice can modify the parameters of the perovskite crystal unit, for instance, embedding La^{3+} ions into $CsPbI_2Br$ perovskite crystal can cause lattice shrinking[88] and the incorporation of Sm^{3+} was found to enhance the binding energy between the rare-earth and Br compared to that of Pb–Br,[84] which contributed to the improvement of moisture stability, enabling air condition processability. Moreover, it was known that Eu^{3+} can be easily reduced to Eu^{2+}. On this basis, Wang and co-workers[89] demonstrated a new concept by introducing redox shuttle in the perovskite thin films using the ionic pair of Eu^{3+}–Eu^{2+}, which can continuously oxidize Pb and reduce I in a cyclical process to avoid the formation of metallic Pb and iodine, as demonstrated in Fig. 11(a). As a result, excellent light stability and thermal stability were obtained, and 90% of the initial PCE can be retained after 8000 h in the Eu doped perovskite device. On the other hand, Feng and co-workers[90] used Eu-porphyrin complex as dopants in the preparation of perovskites. As shown in Fig. 11(b), the porphyrin can interact with PbI_2 to form two-dimensional perovskites within the 3D perovskites and passivate the defect states at the grain boundaries.[91–93] The as-formed 2D–3D hybrid perovskite architecture can significantly boost the device stability when exposed to heating

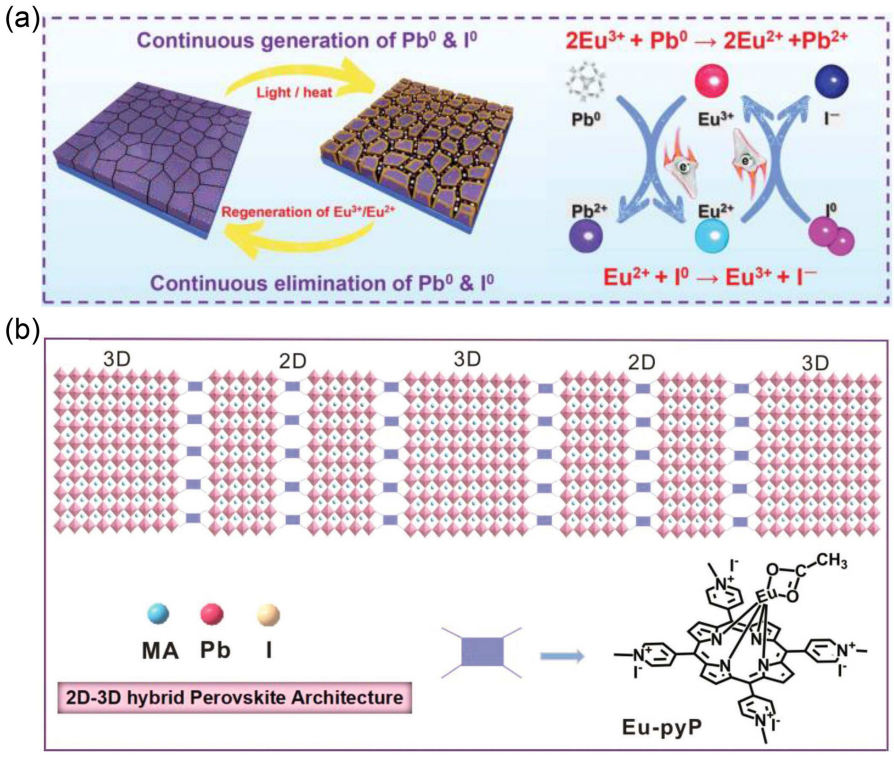


Fig. 11. Perovskite stabilization via rare-earth ions doping. (a) Proposed mechanism diagram of cyclically elimination of Pb and I defects and regeneration of Eu^{3+}–Eu^{2+} metal ion pair;[89] (b) the formation of 2D–3D hybrid perovskite with the assistance of Eu-complex.[90]

and humidity. And also, the incorporation of Eu can significantly boost the light stability of the perovskite device compared to the perovskites using pure porphyrin as dopants. The similar phenomenon can be found by using the Eu–metal–organic framework (MOF) complex.[94] Therefore, the combination of rare-earth elements with other materials or in the format of complex can be used to bring in synergetic effects for synchronous improvement of the resistance against moisture, heat, and UV light.[90] In addition, the perovskite phase stability, especially for inorganic perovskites, can be enhanced by tailoring the grain size into the nanometer range owing to the contribution of surface energy.[95] As aforementioned, the addition of the rare-earth ions into the perovskite precursor can modify the crystallization dynamics and hence the grain size of the as deposited perovskites, to improve the perovskite stability.

4.6. Up-conversion: extending light responsive range

It was well established that some specific rare earth ions can convert near-infrared light into perovskite sensitive light via two-photon or multiphoton up-conversion processes, and numerous investigations have demonstrated their promising application potentials in the mesoporous scaffold layer of perovskite solar cells.[96,97] For instance, the incorporation of some Er ions into the TiO_2 layer can not only regulate the TiO_2 crystal growth, but also convert near infrared light into green light owing to the instinct f–f transitions as illustrated in Fig. 12(b), which can promote the NIR light excitation of perovskite and result in significant enhancement of the photocurrent density of the corresponding perovskite solar cells (Fig. 12(c)).[98] To optimize the up-conversion properties, the co-doping by incorporating some additional rear-earth ions such as Yb^{3+}, etc. into the Er^{3+} doped TiO_2 can enhance the up-conversion efficiency and further broaden the absorption range of the perovskite layer to generate extra photocurrent in the solar cells.[99] In the co-doping system, the Yb^{3+} can be excited by the near infrared incidence radiation with long life time, and the energy can be transferred to the Er^{3+} ions and release as high-energy visible light. Therefore, the combination of different rare-earth ions can adjust the optical properties and conversion efficiency of the up-converting materials. In addition, combining some metal ions into the up-conversion layer together with the rare earth ions can further enhance the up-conversion efficiency.[100,101] For examples, the combinations of the rare earth ions and the metal ions, for examples, Ho^{3+}–Yb^{3+}–Mg^{2+}[102] and Er^{3+}–Yb^{3+}–Li^{+}[103] were employed as dopants to prepare TiO_2, which can boost the up-conversion luminescence to improve the overall efficiency of perovskite solar cells.

Furthermore, the rare-earth containing nanomaterials have also exhibited up-conversion effect and they can be embedded in different layers of perovskite solar cells.[104–108] For examples, β-$NaYF_4$:Yb^{3+}, Er^{3+} nanoparticles[109] or nanoprism[110] were introduced into the TiO_2 as up-conversion layers. Based on the up-conversion effect, part of the near-infrared light was converted into natural visible light, which can then be captured by the photoactive perovskites, thereby improving the utilization rate of solar spectrum and increasing the photocurrent density of the perovskite solar cells. In 2019, Deng and co-workers[111] added an octahedral Li(Gd, Y)F_4:Yb^{3+}, Er^{3+} nanocrystal into the hole transport layer of Spiro-OMeTAD in the perovskite solar cells to broaden the light harvesting. And also, Meng and co-workers[112] directly incorporated β-$NaYF_4$:Yb, Er nanocrystals into the $CH_3NH_3PbI_3$ perovskite layer. It was found that a uniform, dense, high-quality and pinhole-free perovskite film can be obtained in the doped perovskite, which was beneficial for the charge transfer in the photovoltaic device. Moreover, recent investigations have revealed that surface modification is an effective strategy to improve the photovoltaic performance, and the up-conversion materials can also be used as the interface layer in the perovskite solar cells.[113] For examples, Qiu and co-workers[114] applied a thin layer of hydrophobic β-$NaYF_4$:Yb, Er nanoparticles on the top of the perovskite layer, which can fulfill the pinholes of the perovskite films and prevent the penetration of environmental moisture to enhance the device stability. The current density of the optimized perovskite device was obviously improved due to the up-conversion effect of the rare-earth based materials. In 2018, Wu and co-workers[115] successfully incorporated $NaYF_4$:Yb^{3+}, Er^{3+} nanoparticles on top of TiO_2 as a mesoporous layer. The facilitated electron transport from $NaYF_4$:Yb^{3+}, Er^{3+} to TiO_2 and the upconversion properties of $NaYF_4$:Yb^{3+}, Er^{3+} enabled a significant performance improvement of photoelectric conversion efficiency.

However, some parasitically charge recombination can occur when the $NaYF_4$ crystals were directly doped into the perovskite device because of the presence of defects at the $NaYF_4$ surface. To avoid the unintentional defect states, Qi and co-workers[116] designed a core-shell structure of $NaYF_4$:Yb, Er@SiO_2 crystals by using a thin insulating layer of SiO_2 to prevent the direct exposure of $NaYF_4$. The newly optimized up-conversion materials were deposited on the top of the TiO_2 layer, which can not only suppress interfacial non-radiative carrier recombination, but also convert lower-energy NIR photons into visible region and thus enhance the photogenerated current density in the perovskite solar cells. In addition, the up-conversion materials can be used as an independent layer to avoid their contact with the functional layers in perovskite solar cells, for examples, Chen and co-workers[117] introduced a transparent $LiYF_4$:Yb^{3+}, Er^{3+} single crystal as an independent luminescent upconverter in per-

ovskite solar cells to improve light absorption of the solar cells. This transparent single crystal can continue to exert its up-conversion characteristics and convert near-infrared light into visible light.

Although the above up-conversion materials demonstrated promising application potentials to extend the perovskite responsive range, the weak and narrowband absorption of the rare earth ions (Yb^{3+}/Er^{3+}) with spectral window of 10–20 nm in the near-infrared range restricted the overall improvement in device efficiency. Lai and co-workers[118] utilized a hydrophilic IR806 dye-sensitized up-conversion nanocrystal IR806-β-$NaYF_4$:Yb, Er as an interface layer in the perovskite solar cells, which presented a broadband up-conversion of NIR light from 800 nm to 1000 nm into perovskite responsive light emissions (Fig. 12(d)). Therefore, the light sensitive spectra can be broadened by taking advantages of the high extinction coefficient of the organic ligands to effectively sensitize the long-lived f–f transition.[119]

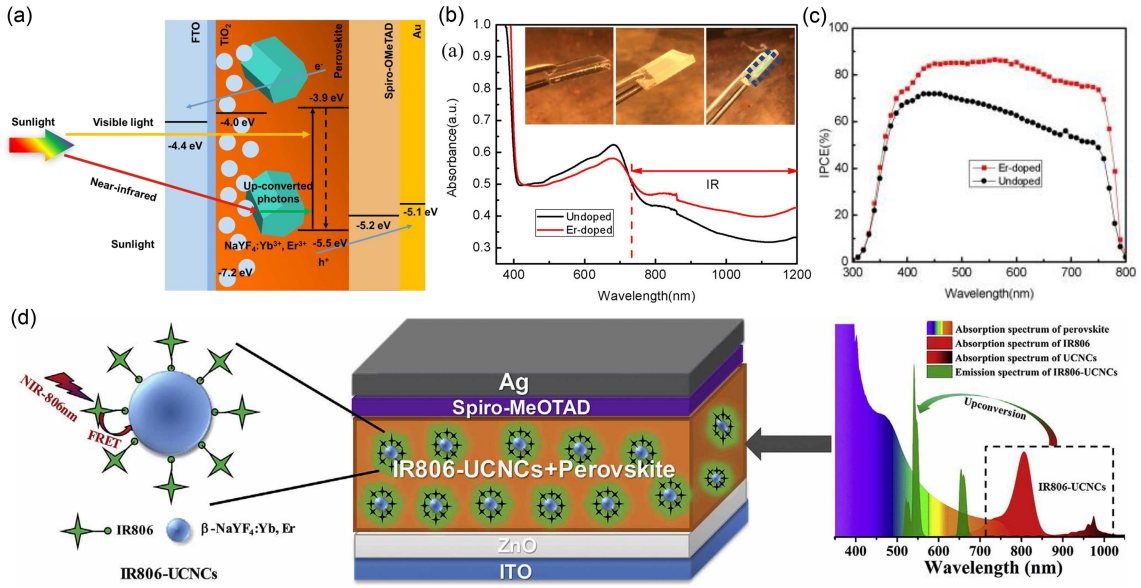


Fig. 12. (a) Schematic illustration of the operational mechanism of perovskite solar cells using up-conversion rare-earth materials, (b) UV-vis absorption spectrum and (c) incident photon-to-electron conversion efficiency (IPCE) spectrum of the perovskite solar cell based on pristine TiO_2 and Er doped TiO_2.[98] (d) Perovskite solar cells using organic dye-sensitized up-conversion nanomaterials with broadband response.[118]

In order to unveil the origin of the photocurrent enhancement, some investigations have revealed that the scattering effect and localized surface plasmon resonance of the incorporated nanoparticles and the optimized light electrical field distribution can contribute to the performance enhancement besides the up-conversion effects.[120,121,123] Nevertheless, the utilization of near-infrared light in the range 800–1100 nm, which is out of the perovskite absorbing range, can be visualized from the external quantum efficiency spectrum and a power conversion efficiency of 0.37% can be obtained when measured under the excitation of 980 nm laser, indicating that the up-conversion effect cannot be ignored and the 980 nm near-infrared light was successfully converted into visible light and be captured by the perovskite.

4.7. Down-conversion: avoiding high energy light damage

Inspired by the luminescent down converting ability of the rare earth materials for UV blocking and conversion, the incorporation of the down-conversion materials into perovskite solar cells can reduce the spectral mismatch losses and avoid the high energy light damage to simultaneously enhance the power conversion efficiency and photostability of the corresponding solar cells. There are two main approaches for the application of down-conversion materials in the perovskite solar cells: one is to introduce the down-conversion materials directly into the functional layers of the perovskite solar cells, and the other one is to deposit an extra layer on the backside of the glass substrates.[124–127]

For examples, Jiang and co-workers[128] used light-emitting materials of Eu^{3+} doped TiO_2, Meng and co-workers[129] doped CeO_x into ZnO to successfully construct a down-converting ETL in perovskite solar cells, respectively. It was shown that, when exposed to solar irradiation, the incident visible light can be directly absorbed by the perovskite layer, and part of the high-energy ultraviolet light is converted into low-energy photons by the down-conversion materials and then absorbed by the perovskite layer, thus improving the photogenerated current density and protecting the perovskite layer from UV light damage in the corresponding solar cells, as illustrated in Fig. 13(a). Similar with the up-conversion materials, combing different rare earth ions can enhance the down-conversion efficiency. For instance, Zhang and co-workers[130] used some additional rare-earth ions in terms of Sm^{3+} and Eu^{3+} to co-dop TiO_2 ETLs in planar $CH_3NH_3PbI_3$ perovskite solar cells, in which the Sm^{3+} is functioned as a sensitizer to capture the high-energy UV photons and transfer the energy to Eu^{3+}, and the Eu^{3+} ions can

convert the captured energy into visible light through down-conversion process. The combination of different rare-earth ions can significantly improve the down-conversion efficiency. Moreover, some rare earth complexes were also used as a functional layer in perovskite solar cells.[131] For instance, the effective luminescent down-conversion materials, such as $Eu(TTA)_2(Phen)MAA$,[132] $CeO_2:Eu^{3+}$ nanophosphors,[125] $Sr_2CeO_4:Eu^{3+}$ nanophosphor[126] were inserted between the ETL and perovskite layer as an interfacial modifier. They demonstrated that the down-conversion of the ultraviolet light can promote light absorption and inhibit the degradation of the device under UV light irradiation. On the other hand, the introduction of the interfacial layer can promote the interface contact and facilitates the transport and collection of electrons, thereby improving the device performance (Fig. 13(b)).

And also, recent investigations have demonstrated that directly coating down-conversion materials on the glass substrates can effectively block and convert the UV light without affecting the intrinsic charge transport and recombination.[99,133,134] For examples, Jiang and co-workers[127] employed a layer of Eu−4,7-diphenyl-1,10-phenanthroline (Eu-complex) on the backside of the fluorine-doped tin oxide (FTO) glass as down-converting layer (DCL) (Fig. 13(c)). Compared with the pristine perovskite solar cells, the application of such DCL displayed an obvious enhancement of 11.8% in short-circuit current density (J_{SC}) and 15.3% in efficiency because of the conversion of UV light (300–380 nm) into the perovskite responsive wavelength range. Moreover, the photostability of the optimized device under UV light was significantly enhanced owing to the UV blocking effect (Fig. 13(d)). Similarly, Jia and co-workers[135] deposited an extra layer of $NaYF_4:Eu^{3+}$ down-conversion nanocrystals on the back of the FTO coated glass substrates. Zhang and co-workers[136] successfully prepared Sm^{3+} and Ce^{3+} ions co-doped P_2O_5-Li_2O-ZnO-Sm_2O_3-CeO_2 glass-ceramic waveguide as the glass substrates for perovskite solar cells. In such case, under an operational condition, the UV light is firstly filtered by the down-conversion layer and converted into low-energy photons, which can not only expand the spectral response range but also avoid the photocatalytic activity of the TiO_2, thereby improving the photogenerated current and operational stability of the perovskite solar cells. More interestingly, according to the promising up-converting and down-converting properties, full spectrum responsive perovskite solar cells are desirable by convert UV and NIR light to visible light in one device, as illustrated in Figs. 14(a) and 14(b).[137]

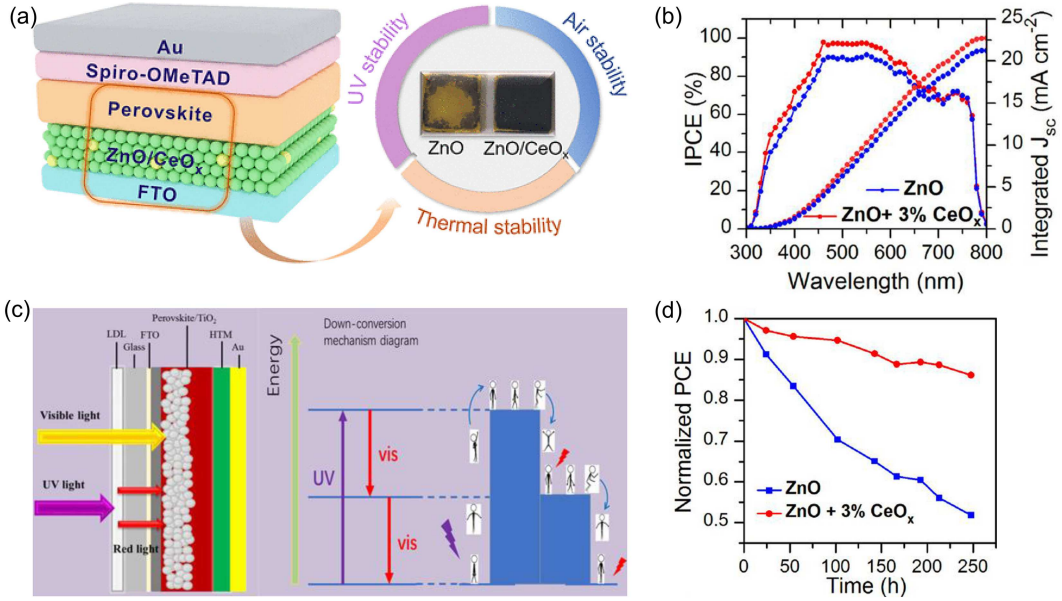


Fig. 13. (a) Device structure of perovskite solar cells employing a down-conversion layer.[129] (b) IPCE spectra and integrated J_{SC}, for the pristine and down-conversion materials doped perovskite solar cells.[129] (c) Schematic illustration of down-conversion mechanism in perovskite solar cells,[127] (d) long term stability of the pristine and down-conversion materials doped perovskite.[129]

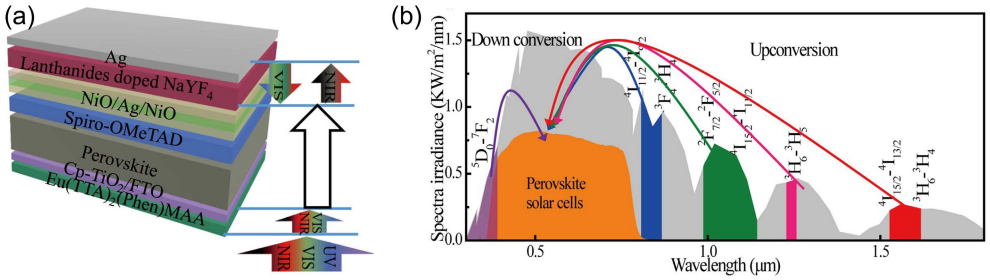


Fig. 14. (a) Device structure of full spectrum response perovskite solar cells and (b) the spectral regions in solar spectrum by perovskite solar cells that utilized up-conversion and down-conversion materials.[137]

5. Conclusion and perspectives

In summary, state-of-the-art perovskite solar cells suffer from defect assisted non-radiative recombination, light induced degradation and mismatch between absorption and solar spectrum, seriously restricting their power conversion efficiency and operational stability. It has been previously revealed that the rare-earth ions can be coupled with charge transport metal oxides and perovskite layers, and the aforementioned issues can be effectively mitigated by taking advantages of the unique property of rare-earth ions, resulting in improved power conversion efficiency as summarized in Table 1. The functions of the rare-earth ions in perovskite solar cells can be understood from the following aspects: (1) optimizing charge transport layers with reduced defect states, enhanced charge mobility and aligned energy level; (2) modifying the morphology of metal oxide thin films to avoid the nanoparticle aggregation and pin-hole formation, and to regulate nanostructure of the metal oxides for scaffold layers; (3) tuning photophysical property of perovskites via substitutional or interstitial doping to reduce trap defects and boost the light harvesting and luminescence; (4) regulating perovskite crystallization with optimized thin film morphology and lowered formation energy via the strong interaction between the rare-earth ions and charged ions in the precursor; (5) stabilizing perovskite phase structure with eliminated defect states, tailored grain size, modified lattice parameters and rendered redox capability; (6) extending light responsive range by converting the UV light and NIR light into perovskite responsive visible light via the incorporation of up-conversion or down-conversion rare-earth nanomaterials; (7) avoiding high energy light damage via UV light blocking to enhance the operational stability of the perovskite solar cells.

Table 1. Performance comparison of the pristine perovskite solar cells and the rare-earth ions doped device.

Dopants	Device structure & dopant position (highlighted)	V_{OC} (V)	J_{SC} (mA·cm^{-2})	FF (%)	PCE (%)	Ref.
Y	FTO/cTiO$_2$/mp-TiO$_2$/perovskite/Spiro-OMeTAD/Au	0.94	15.8	70	10.5	[47]
		0.95	18.1	66	11.2	
La	FTO/bl-TiO$_2$/mp-TiO$_2$/MAPbI$_3$/Spiro-OMeTAD/Au	1.00	20.28	60	12.1	[43]
		1.05	21.30	69	15.4	
Sm	FTO/c-TiO$_2$/MAPbI$_3$/Spiro-OMeTAD/Au	1.03	18.1	68.3	12.8	[44]
		1.04	19.1	70.6	14.1	
Eu	FTO/bl-TiO$_2$/mp-TiO$_2$/MAPbI$_3$/Spiro-OMeTAD/Au	1.01	22.0	67.9	15.9	[45]
		1.10	22.6	72.3	17.9	
Nd	FTO/c-TiO$_2$/mp-TiO$_2$/perovskite/Spiro-OMeTAD/Au	1.13	22.0	69.7	17.3	[42]
		1.13	22.3	71.6	18.1	
Er	FTO/c-TiO$_2$/mp-TiO$_2$/MAPbI$_3$/Spiro-OMeTAD/Au	0.91	18.4	57.5	9.6	[56]
		1.03	20.3	67.3	14.1	
Er-Yb	FTO/c-TiO$_2$/mp-TiO$_2$/MAPbI$_{3x}$Cl$_x$/Spiro-OMeTAD/Au	0.80	20.4	63	10.3	[99]
		0.87	21.7	66	12.9	
Mg/Er	FTO/cTiO$_2$/Cs$_{0.05}$(MA$_{0.17}$FA$_{0.83}$)$_{0.95}$Pb(I$_{0.83}$Br$_{0.17}$)$_3$	1.05	21.4	75	17.1	[138]
	/Spiro-OMeTAD/Au	1.07	23.2	76	19.0	
β-NaYF$_4$:Yb^{3+}, Er^{3+}@SiO$_2$	FTO/c-TiO$_2$/mp-TiO$_2$/ZrO$_2$/ MAPbI$_3$/C	0.97	16.57	51	8.19	[72]
		0.93	19.72	54	9.92	
Sc^{3+}, Y^{3+}, La^{3+}	FTO/SnO$_2$/perovskite/Spiro- OMeTAD/Au	1.11	23.1	74.5	19.0	[74]
		1.12	23.6	78.2	20.6	
La	FTO/NiO$_x$/MAPbI$_3$/PC$_{61}$BM/BCP/Ag	0.99	18.8	66.7	12.3	[64]
		1.02	20.3	73.1	15.0	
Y	FTO/NiO$_x$/MAPbI$_3$/ PC$_{61}$BM/Ag	0.96	23.3	57	12.8	[68]
		1.00	23.8	68	16.3	
Ce, Nd, Eu, Tb, and Yb	FTO/NiO$_x$/MAPbI$_3$/ PCBM/Ag	1.00	18.1	66.6	12.2	[48]
		1.03	22.0	66.6	15.1	
Y	FTO/SnO$_2$/MAPbI$_3$/Spiro-OMeTAD/Au	1.05	19.3	66	13.4	[71]
		1.08	22.6	71	17.3	
EuI$_2$	FTO/NiO/MAPbI$_3$/PCBM/Ag	1.02	19.2	67.8	13.3	[75]
		1.02	21.5	76.4	16.7	
Eu^{3+}-Eu^{2+}Eu(acac)$_3$	ITO/TiO$_2$/perovskite/Spiro-OMeTAD/Au					[89]
		1.15	23.5	80.7	21.9	
Eu-porphyrin complex	FTO/c-TiO$_2$/mp-TiO$_2$/MAPbI$_3$ /Spiro-OMeTAD/Au	1.09	23.0	75.6	19.0	[90]
		1.08	22.7	74.9	18.4	
EuCl$_3$	FTO/c-TiO$_2$/m-TiO$_2$/CsPbI$_3$ /Spiro-OMeTAD/Au					[87]
		0.898	11.1	0.68	6.8	
EuI$_2$	FTO/TiO$_2$/CsPb$_{0.95}$Eu$_{0.05}$I$_2$Br /Spiro-OMeTAD/Au	1.12	12.6	72.5	10.2	[80]
		1.22	14.6	76.6	13.7	
Eu(Ac)$_3$	FTO/TiO$_2$/CsPbI$_2$Br/Spiro-OMeTAD/Au	1.18	15.4	78.2	14.3	[81]
		1.25	15.4	79.0	15.3	
Sm^{3+}	FTO/c-TiO$_2$/mp-TiO$_2$/ CsPb$_3$Br$_3$/carbon	1.35	6.94	74.5	6.99	[84]
		1.59	7.48	85.1	10.1	
β-NaYF$_4$:Yb^{3+}/Er^{3+}	FTO/c-TiO$_2$/mp-TiO$_2$/(FA$_{0.83}$MA$_{0.17}$)$_{0.95}$Cs$_{0.05}$Pb(I$_{0.9}$Br$_{0.1}$)$_3$	1.14	21.4	71.5	17.4	[37]
/Sc^{3+}@NaYF$_4$	/Spiro-OMeTAD/Au	1.14	22.9	77.0	20.2	
Er$_2$(SO$_4$)$_3$8H$_2$O	FTO/TiO$_2$/CH$_3$NH$_3$PbI$_{3-x}$Cl$_x$/Ag	0.73	19.2	65	9.1	[98]
		0.67	23.0	69	10.6	
Ho^{3+}-Yb^{3+}-Mg^{2+}	FTO/TiO$_2$/perovskite/Spiro-OMeTAD/Au	1.03	21.2	69.6	15.2	[102]
		1.05	22.6	68.7	16.3	

Table 1. continued.

Dopants	Device structure & dopant position (highlighted)	V_{OC} (V)	J_{SC} (mA·cm^{-2})	FF (%)	PCE (%)	Ref.
Er^{3+}-Yb^{3+}-Li^{+}	FTO/TiO_2/perovskite/Spiro-OMeTAD/Au	1.01	21.0	66.0	14.0	[103]
		1.05	22.2	70.8	16.5	
β-$NaYF_4$:Yb, Er	FTO/cm-ZnO/$MAPbI_3$/Spiro-OMeTAD/Ag	1.13	18.7	63.9	13.5	[112]
		1.15	22.7	75.4	19.7	
Li(Gd,Y)F_4:Yb, Er	FTO/c-TiO_2/mp-TiO_2/$MAPbI_3$ /Spiro-OMeTAD/Au	1.06	20.8	66.7	14.7	[111]
		1.10	23.1	72.1	18.3	
NYF@TiO_2	FTO/c-TiO_2/perovskite/Spiro-OMeTAD/Ag	1.08	20.1	65.0	13.8	[109]
		1.10	21.7	70.6	16.9	
IR806-$NaYF_4$:Yb, Er	FTO/cm-ZnO/$MAPbI_3$/Spiro-OMeTAD/Ag	1.11	18.4	66.2	13.5	[118]
		1.12	22.0	71.1	17.5	
β-$NaYF_4$:Yb^{3+}, Er^{3+}	FTO/cm-TiO_2/mp-TiO_2/$MAPbI_3$/Spiro-OMeTAD/Au	1.09	18.9	0.68	14.1	[110]
		1.10	20.2	0.72	16.0	
$NaYF_4$:Yb^{3+}, Er^{3+}	FTO/bl-TiO_2/mp-TiO_2/$MAPbI_3$/HTM/Au	1.04	19.2	75.8	15.2	[115]
		1.06	21.3	76.7	17.3	
SiO_2/$NaYF_4$:Yb,Er@SiO_2	FTO/cm-TiO_2/SiO_2/$NaYF_4$:Yb, Er@SiO_2/$MAPbI_3$/C	0.971	20.6	59.3	11.9	[116]
		1.02	21.3	64.6	14.0	
CeO_2:Eu^{3+}	FTO/c-TiO_2/CeO_2:Eu^{3+}m-TiO_2/$MAPbI_3$	0.88	19.2	59.8	10.1	[125]
	/Spiro-OMeTAD/Ag	0.90	20.5	58.7	10.8	
Eu^{3+} crystal	FTO/TiO_2:Eu^{3+}crystal/$MAPbI_3$/Spiro-OMeTAD/Au	1.00	17.0	71.3	12.2	[128]
		1.08	19.3	75.7	15.8	
Sm^{3+}, Eu^{3+}	FTO/TiO_2/$MAPbI_3$/Spiro-OMeTAD/Ag	1.06	22.2	74.7	17. 6	[130]
		1.10	22.5	76.9	19.0	
$Eu(TTA)_2(Phen)MAA$	FTO/TiO_2/mp-TiO_2/perovskite /Spiro-OMeTAD/Au	1.06	22.0	72.8	17.0	[132]
		1.08	23.2	76.0	19.1	
CeO_x	FTO/ZnO/CeO_x/$MAPbI_3$/Spiro-OMeTAD/Au	1.02	22.1	71.2	16.0	[129]
		1.09	23.6	75.7	19.5	
Sr_2CeO_4:Eu^{3+} (SCOE)	FTO/c-TiO_2/SCOE/(CsFAMA) $Pb(BrI)_3$	1.04	21.8	73.4	16.6	[126]
	/Spiro-OMeTAD/Au	1.06	23.7	75.5	19.0	
Eu-complex LDL	LDL/FTO/c-TiO_2/mp-TiO_2/ $MAPbI_3$/Spiro-OMeTAD /Au	1.03	17.3	73.5	13.1	[127]
		1.05	19.3	76.0	15.4	
$NaYF_4$:Eu^{3+}	$NaYF_4$:Eu^{3+}/FTO/TiO_2/$Cs_{0.05}(MA_{0.17}FA_{0.83})_{0.95}Pb(I_{0.83}Br_{0.17})_3$	1.11	21.3	75.0	17.7	[135]
	/Spiro-OMeTAD/Au	1.13	23.2	77.1	20.2	
Sm^{3+}, Ce^{3+}	FTO:Sm^{3+}, Ce^{3+}/PSC/metal back reflector	0.82	16.3	53.4	7.1	[136]
		0.82	17.9	53.4	7.8	

Although the rare-earth ions have exhibited a very broad application prospect in perovskite solar cells and some aggressive progresses have been achieved, it is still a big challenge to effectively boost the device efficiency and stability. Further efforts should be focused on the following aspects: (1) the synthesis of diverse and efficient nanomaterials based on rare-earth ions to bring in synergistic effects from both the rare-earth ions and the counterparts; (2) strategies to eliminate the parasitic charge recombination when incorporating the rare-earth ions as additives in the perovskite device;[139] (3) the conversion efficiency, absorption cross-sectional area and responsive spectral range of the up-conversion materials and down-conversion materials need to be further improved;[140] (4) the *B* site in the perovskite lattice can be substituted by rare-earth ions for the fabrication of lead free perovskites to avoid the toxicity issues of Pb, perovskites such as $CsYbI_3$,[141] $CsEuBr_3$,[142] $CsEuCl_3$,[143] $CsEuI_3$ and $CH_3NH_3EuI_3$[144] have been successfully synthesized with promising optoelectronic properties, but their applications in photovoltaic device have not been explored.

Acknowledgments

Project supported by the National Key R&D Program of China (Grant No. 2020YFA07099003), Six Talent Peaks Project of Jiangsu Province, China (Grant No. 2019-XNY-013), and a fellowship from the China Postdoctoral Science Foundation (Grant No. 2020M672181).

References

[1] Kojima A, Teshima K, Shirai Y and Miyasaka T 2019 *J. Am. Chem. Soc.* **131** 6050
[2] Wang J F, Lin D X and Yuan Y B 2019 *Acta Phys. Sin.* **68** 158801 (in Chinese)
[3] Hou S, Shi B, Wang P, Li Y, Zhang J, Chen P, Chen B, Hou F, Huang Q, Ding Y, Li Y, Zhang D, Xu S, Zhao Y and Zhang X 2020 *Chin. Phys. B* **29** 078801
[4] Xia J M, Liang C and Xing G C 2019 *Acta Phys. Sin.* **68** 158807 (in Chinese)
[5] Liang Z, Yang B, Mei A, Lin S, Han H, Yuan Y, Xie H, Gao Y and Zhou C 2020 *Chin. Phys. B* **29** 078401
[6] Yang J, Zhang P, Wang J and Wei S H 2020 *Chin. Phys. B* **29** 108401
[7] Wang J M, Chen K, Xie W G, Shi T T, Liu P Y, Zheng Y F and Zhu R 2019 *Acta Phys. Sin.* **68** 158806 (in Chinese)
[8] Hui W, Chao L F, Lu H, Xia F, Wei Q, Su Z, Niu T, Tao L, Du B, Li D, Wang Y, Dong H, Zuo S, Li B, Shi W, Ran X, Li P, Zhang H, Wu Z, Ran C, Song L, Xing G, Gao X, Zhang J, Xia Y, Chen Y and Huang W 2021 *Science* **371** 1359
[9] Oregan B and Gratzel M 1991 *Nature* **353** 737
[10] Kim S H, Lee C R,Im J H, Lee K B, Moehl T, Marchioro A, Moon S J, Humphry Baker R, Yum J H, Moser J E, Grätzel M and Park N G 2012 *Sci. Rep.* **2** 591
[11] https://www.nrel.gov/pv/assets/pdfs/best-research-cellefficiencies.20200104.pdf accessed on April 1, 2021
[12] Zhang H and Toudert J 2018 *Sci. Technol. Adv. Mat.* **19** 411
[13] Zhang H, Kramarenko M, Osmond J, Toudert J and Martorell J 2018 *ACS Photonics* **5** 2243
[14] Wang J P, Zhang H, Wang L, Yang K, Cang L M, Liu X and Huang W 2020 *ACS Appl. Energy Mater.* **3** 4484

[15] Peng J, Walter D, Ren Y, Tebyetekerwa M, Wu Y, Duong T, Lin Q, Li J, Lu T, Mahmud M A, Lem O L C, Zhao S, Liu W, Liu Y, Shen H, Li L, Kremer F, Nguyen H T, Choi D Y, Weber K J, Catchpole K R and White T P 2021 *Science* **371** 390

[16] Frost J M, Butler K T, Brivio F, Hendon C H, Van Schilfgaarde M and Walsh A 2014 *Nano Lett.* **14** 2584

[17] Yu Z and Sun L C 2015 *Adv. Energy Mater.* **5** 1500213

[18] Li W Z, Li J W, Niu G D and Wang L D 2016 *J. Mater. Chem. A* **4** 11688

[19] Li W Z, Zhang W, Van Reenen S, Sutton R J, Fan J D, Haghighirad A A, Johnston M B, Wang L D and Snaith H J 2016 *Energy Environ. Sci.* **9** 490

[20] Lv Y F, Zhang H, Liu R Q, Sun Y N and Huang W 2020 *ACS Appl. Mater. Interfaces* **12** 27277

[21] Lv Y F, Xu P H, Ren G Q, Chen F, Nan H R, Liu R Q, Wang D, Tan X, Liu X Y, Zhang H and Chen Z K 2018 *ACS Appl. Mater. Interfaces* **10** 23928

[22] Lluscà N, Lopez-Vidrier J, Lauzurica S, Sanchez-Aniorte M I, Antony A, Molpeceres C, Hernández S, Garrido B and Bertomeu J 2015 *J. Lumin.* **167** 101

[23] Huang X Y, Han S Y, Huang W and Liu X G 2013 *Chem. Soc. Rev.* **42** 173

[24] Wang H Q, Batentschuk M, Osvet A,Pinna L and Brabec C J 2011 *Adv. Mater.* **23** 2675

[25] Tyler G 2004 *Plant Soil* **267** 191

[26] Chen X, Wang W J, Chen X Y, Bi J H, Wu L, Li Z H and Fu X Z 2009 *Mater. Lett.* **63** 1023

[27] Grosjean N, Le Jean M, Berthelot C, Chalot M, Gross E M and Blaudez D 2019 *Sci. Rep.* **9** 18458

[28] Kolesnikov I E, Kalinichev A A, Kurochkin M A, Golyeva E V, Terentyeva A S, Kolesnikov E Y and Lahderanta E 2019 *Sci. Rep.* **9** 2043

[29] Stranks S D, Eperon G E, Grancini G, Menelaou C, Alcocer M J P, Leijtens T, Herz L M, Petrozza A and Snaith H J 2013 *Science* **342** 341

[30] Auzel F 2004 *Chem. Rev.* **104** 139

[31] Wang F and Liu X G 2009 *Chem. Soc. Rev.* **38** 976

[32] Hou X, Xuan T T, Sun H C, Chen X H, Li H L and Pan L K 2016 *Sol. Energy Mater. Sol. Cells* **149** 121

[33] Auzel F 2005 *Spectrosc. Prop. Rare Earths Opt. Mater.* **83** 266

[34] Chen Y H, Liu S C, Zhou N, Li N X, Zhou H P, Sun L D and Yan C H 2021 *Prog. Mater. Sci.* **120** 100737

[35] Qiao Y, Li S H, Liu W H, Ran M Q, Lu H F and Yang Y P 2018 *Nanomater.* **8** 43

[36] Ma X H, Yang L Q, Lei K X, Zheng S J, Chen C and Song H W 2020 *Nano Energy* **78** 105354

[37] Guo Q Y, Wu J H, Yang Y Q, Liu X P, Jia J B, Dong J, Lan Z, Lin J M, Huang M L, Wei Y L and Huang Y F 2019 *J. Power Sources* **426** 178

[38] Yoo J J, Seo G, Chua M R, Park T G, Lu Y L, Rotermund F, Kim Y K, Moon C S, Jeon N J, Correa Baena J P, Bulovic V, Shin S S, Bawendi M G and Seo J 2021 *Nature* **590** 7847

[39] Qian Z Y, Chen L B, Wang J P, Wang L, Xia Y D, Ran X Q, Li P, Zhong Q, Song L, Muller Buschbaum P, Chen Y H and Zhang H 2021 *Adv. Mater. Interfaces* **8** 2100128

[40] Chen X B and Mao S S 2007 *Chem. Rev.* **107** 2891

[41] Pathak S K, Abate A, Ruckdeschel P, Roose B, Gödel K C, Vaynzof Y, Santhala A, Watanabe S I, Hollman D J, Noel N, Sepe A, Wiesner U, Friend R, Snaith H J and Steiner U 2014 *Adv. Funct. Mater.* **24** 6046

[42] Roose B, Godel K C, Pathak S, Sadhanala A, Baena J P C, Wilts B D, Snaith H J, Wiesner U, Gratzel M, Steiner U and Abate A 2016 *Adv. Energy Mater.* **6** 1501868

[43] Gao X X, Ge G G, Xue D J, Ding J, Ma J Y, Chen Y X, Zhang B, Feng Y Q, Wan L J and Hu J S 2016 *Nanoscale* **8** 16881

[44] Xiang Y, Ma Z, Zhuang J, Lu H L, Jia C Y, Luo J S, Li H M and Cheng X W 2017 *J. Phys. Chem. C* **121** 20150

[45] Xu Z, Wu J H, Wu T Y, Bao Q L, He X, Lan Z, Lin J M, Huang M L, Huang Y F and Fan L Q 2017 *Energy Technol.* **5** 1820

[46] Zhou H P, Chen Q, Li G, Luo S, Song T B, Duan H S, Hong Z R, You J B, Liu Y S and Yang Y 2014 *Science* **345** 542

[47] Qin P D, Domanski A L, Chandiran A K, Berger R, Butt H J, Dar M I, Moehl T, Tetreault N, Gao P, Ahmad S, Nazeeruddin M K and Grätzel M 2014 *Nanoscale* **6** 1508

[48] Chen X F, Xu L, Chen C, Wu Y J, Bi W B, Song Z L, Zhuang X M, Yang S, Zhu S D and Song H W 2019 *J. Power Sources* **444** 227267

[49] Jiang Q, Zhang X W and You J B 2018 *Small* **14** 1801154

[50] Song J, Zhang W N, Wang D, Deng K M, Wu J H and Lan Z 2019 *Sol. Energy* **185** 508

[51] Liu X, Zhang Y F, Shi , Liu Z H, Huang J F, Yun J S, Zeng Y Y, Pu A B, Sun K W, Hameiri Z, Stride J A, Seidel J, Green M A and Hao X 2018 *Adv. Energy Mater.* **8** 1800138

[52] Anaraki E H, Kermanpur A, Mayer M T, Steier L, Ahmed T, Turren Cruz S H, Seo J, Luo J, Zakeeruddin S M, Tress W R, Edvinsson T, Grätzel M, Hagfeldt A and Correa Baena J P 2018 *ACS Energy Lett.* **3** 773

[53] Ren X D, Yang D, Yang Z, Feng J S, Zhu X J, Niu J Z, Liu Y Z, Zhao W G and Liu S F 2017 *ACS Appl. Mater. Interfaces* **9** 2421

[54] Chen J Z, Yang H B, Tao H B, Zhang L P, Miao J W, Wang H Y, Chen J Z, Zhang H and Liu B 2016 *Adv. Funct. Mater.* **26** 456

[55] Gao Y Y, Zhu J, An H Y, Yan P L, Huang B K, Chen, R T, Fan F T and Li C 2017 *J. Phys. Chem. Lett.* **8** 1419

[56] Ren Z Q, Wu J D, Wang N and Li X 2018 *J. Mater. Chem. A* **6** 15348

[57] Park J H, Seo J, Park S, Shin S S, Kim Y C, Jeon N J, Shin H W, Ahn T K, Noh J H, Yoon S C, Hwang C S and Seok S I 2015 *Adv. Mater.* **27** 4013

[58] Zhu Z L, Bai Y, Zhang T, Liu Z K, Long X, Wei Z H, Wang Z L, Zhang L X, Wang J N, Yan F and Yang S H 2014 *Angew. Chem.* **53** 12571

[59] You J B, Meng L, Song T B, Guo T F, Yang Y, Chang W H, Hong Z R, Chen H J, Zhou H P, Chen Q, Liu Y S and De Marco N 2016 *Nat. Nanotechnol.* **11** 75

[60] Zhang K H L, Xi K, Blamire M G and Egdell R G 2016 *J. Phys.: Condens. Matter* **28** 383002

[61] Zhang W B, Yu N, Yu W Y and Tang B Y 2008 *Eur. Phys. J. B* **64** 153

[62] Bai Y, Chen H N, Xiao S, Xue Q F, Zhang T, Zhu Z L, Li Q, Hu C, Yang Y, Hu Z C, Huang F, Wong K S, Yip H L and Yang S 2016 *Adv. Funct. Mater.* **26** 2950

[63] Chen W, Wu Y Z, Yue Y F, Liu J, Zhang W J, Yang X D, Chen H, Bi E B, Ashraful I, Gratzel M and Han L Y 2015 *Science* **350** 944

[64] Teo S, Guo Z L, Xu Z H, Zhang C, Kamata Y, Hayase S and Ma T L 2019 *ChemSusChem* **12** 518

[65] Lin J and Yun J C 1998 *J. Photochem. Photobiol. A* **116** 63

[66] Xu A W, Gao Y and Liu H Q 2002 *J. Catal.* **207** 151

[67] Abu Zied B M, Bawaked S M, Kosa S A and Schwieger W 2016 *Catalysts* **6** 70

[68] Hu Z J, Chen D, Yang P, Yang L J, Qin L H, Huang Y H and Zhao X C 2018 *Appl. Surf. Sci.* **441** 258

[69] Xu Y N, Gu Z Q and Ching W Y 1997 *Phys. Rev. B* **56** 14993

[70] Zhao B X, Wang, J S, Li H Y, Wang H, Jia X J and Su P L 2015 *Phys. Chem. Chem. Phys.* **17** 14836

[71] Xu Z H, Teo S H, Gao L G, Guo Z L, Kamata Y, Hayase S and Ma T L 2019 *Org. Electron.* **73** 62

[72] Yang G, Lei H W, Tao H, Zheng X L, Ma J J, Liu Q, Ke W J, Chen Z L, Xiong L B, Qin P L, Chen Z, Qin M C, Lu X H, Yan Y F and Fang G J 2017 *Small* **13** 1601769

[73] Liu B and Aydil E S 2009 *J. Am. Chem. Soc.* **131** 3985

[74] Guo Q Y, Wu J H, Yang Y Q, Liu X P, Lan Z, Lin J M, Huang M L, Wei Y L, Dong J, Jia J B and Huang Y F 2019 *Research* **2019** 4049793

[75] Wu X W, Li H W, Wang K, Sun X W and Wang L D 2018 *RSC Adv.* **8** 11095

[76] Pan G C, Bai X, Yang D W, Chen X, Jing P T, Qu S N, Zhang L J, Zhou D L, Zhu J Y, Xu W, Dong B and Song H W 2017 *Nano Lett.* **17** 8005

[77] Suzuki A and Oku T 2021 *Mater. Adv.* **2** 2609

[78] Yin J, Ahmed G H, Bakr O M, Bredas J L and Mohammed O F 2019 *Acs Energy Lett.* **4** 789

[79] Li X Y, Duan S, Liu H C, Chen G Y, Luo Y and Agren H 2019 *J. Phys. Chem. Lett.* **10** 487

[80] Xiang W C, Wang Z W, Kubicki D J, Tress W, Luo J S, Prochowicz D, Akin S, Emsley L, Zhou J T, Dietler G, Gratzel M and Hagfeldt A 2019 *Joule* **3** 205

[81] Yang S M, Zhao H, Han Y, Duan C Y, Liu L K and Liu S Z 2019 *Small* **15** e1904387

[82] Chen L B, Wu W, Wang J P, Qian Z Y, Liu R G, Niu Y Y, Chen Y H, Xie X J and Zhang H 2021 *ACS Appl. Energy Mater.* **4** 3937

[83] Xiang W C, Wang Z W, Kubicki D J, Tress W, Luo J S, Prochowicz D, Akin S, Emsley L, Zhou J T, Dietler G, Gratzel M and Hagfeldt A 2019 *Joule* **3** 205

[84] Duan J L, Zhao Y, Yang X Y, Wang Y D, He B L and Tang Q W 2018 *Adv. Energy Mater.* **8** 1802346

[85] Eperon G E, Paternò G M, Sutton R J, Zampetti A, Haghighirad A A, Cacialli F and Snaith H J 2015 *J. Mater. Chem. A* **3** 19688
[86] Wang J P, Chen L B, Qian Z Y, Ren G Q, Wu J and Zhang H 2020 *J. Mater. Chem. A* **8** 25336
[87] Jena A K, Kulkarni A, Sanehira Y, Ikegami M and Miyasaka T 2018 *Chem. Mater.* **30** 6668
[88] Chen S L, Zhang T J, Liu X L, Qiao J L, Peng L, Wang J, Liu Y S, Yang T Y and Lin J 2020 *J. Mater. Chem. C* **8** 3351
[89] Wang L G, Zhou H P, Hu J N, Huang B L, Sun M Z, Dong B W, Zheng G H J, Huang Y, Chen Y H, Li L, Xu Z Q, Li N X, Liu Z, Chen Q, Sun L D and Yan C H 2019 *Science* **363** 265
[90] Feng X X, Chen R H, Nan Z A, Lv X D, Meng R Q, Cao J and Tang Y 2019 *Adv. Sci.* **6** 1802040
[91] Gao K, Zhu Z L, Xu B, Jo S B, Kan Y Y, Peng X B and Jen A K 2017 *Adv. Mater.* **29** 1703980
[92] Cao J, Lv X D, Zhang P, Chuong T T, Wu B H, Feng X X, Shan C F, Liu J C and Tang Y 2018 *Adv. Mater.* **30** 1800568
[93] Xia H Q, Wang J, Jia R, Wang Q and Zhang H X 2015 *Chem. Res. Chin. Univ.* **31** 276
[94] Dou J, Zhu C, Wang H, Han Y, Ma S, Niu X X, Li N X, Shi C B, Qiu Z W, Zhou H P, Bai Y and Chen Q 2021 *Adv. Mater.* **33** 2102947
[95] Yang Y, Han D W, Yang Y, Yi S W, Yuan Q, Zhou D Y and Feng L 2020 *APL Mater.* **8** 071102
[96] He M, Pang X C, Liu X Q, Jiang B B, He Y J, Snaith H J and Lin Z Q 2016 *Angew. Chem.* **55** 4280
[97] Liang J W, Gao H P, Yi M J, Shi W J, Liu Y F, Zhang Z L and Mao Y L 2017 *Electrochim. Acta* **261** 14
[98] Zhang H, Zhang Q S, Lv Y Q, Yang C, Chen H H and Zhou X F 2018 *Mater. Res. Bull.* **106** 346
[99] Wang X L, Zhang Z L, Qin J Q, Shi W J, Liu Y F, Gao H P and Mao Y L 2017 *Electrochim. Acta* **245** 839
[100] Cao B S, He Y Y, Sun Y, Song M and Dong B 2011 *J. Nanosci. Nanotechnol.* **11** 9899
[101] He Y Y, Wu J L, Wang X H, Feng Z Q and Dong B 2016 *J. Nanosci. Nanotechnol.* **16** 3768
[102] Zhang Z L, Li D N, Shi W J, Liu Y Y, Zhang Y, Liu Y F, Gao H P and Mao Y L 2018 *Nanoscale Res. Lett.* **13** 262
[103] Zhang Z L, Qin J Q, Shi W J, Liu Y Y, Zhang Y, Liu Y F, Gao H P and Mao Y L 2018 *Nanoscale Res. Lett.* **13** 147
[104] Green M A and Bremner S P 2016 *Nat. Mater.* **16** 23
[105] Trupke T, Green M A and Wurfel P 2002 *J. Appl. Phys.* **92** 1668
[106] Wang G F, Peng Q and Li Y D 2011 *Acc. Chem. Res.* **44** 322
[107] Dong A G, Ye X C, Chen J, Kang, Y J, Gordon T, Kikkawa J M and Murray C B 2011 *J. Am. Chem. Soc.* **133** 998
[108] Shin J, Kim Y, Lee J, Kim S and Jang H S 2017 *Part. Part. Syst. Charact.* **34** 1600183
[109] Que M D, Que W H, Yin X G, Chen P, Yang Y W, Hu J X, Yu B Y and Du Y P 2016 *Nanoscale* **8** 14432
[110] Roh J, Yun H and Jang J 2016 *ACS Appl. Mater. Interfaces* **8** 19847
[111] Deng X H, Zhang C X, Zheng J F, Zhou X, Yu M D, Chen X H and Huang S M 2019 *Appl. Surf. Sci.* **485** 332
[112] Meng F L, Wu J J, Zhao E F, Zheng Y Z, Huang M L, Dai L M, Tao X and Chen J F 2017 *Nanoscale* **9** 18535
[113] Rajeswari R, Susmitha K, Jayasankar C K, Raghavender M and Giribabu L 2017 *Sol. Energy* **157** 956
[114] Qiu L , Yang Y, Dong G H, Xia D B, Li M R, Fan X and Fan R Q 2018 *Appl. Surf. Sci.* **448** 145
[115] Wu Y H, Ding X H, Shi X Q, Hayat T, Alsaedi A, Ding Y, Mo L E and Dai S Y 2018 *ACS Sustainable Chem. Eng.* **6** 14004
[116] Qi F, Xiao Y Q, Yu Z H, Liu P, Kong S, Li F J, Zhang H J, Wang Y and Zhao X Z 2019 *Org. Electron.* **73** 152
[117] Chen X, Xu W, Song H W, Chen C, Xia H P, Zhu Y S, Zhou D L, Cui S B, Dai Q L and Zhang J Z 2016 *ACS Appl. Mater. Interfaces* **8** 9071
[118] Lai X S, Li X T, Lv X D, Zheng Y Z, Meng F L and Tao X 2017 *J. Power Sources* **372** 125
[119] Ferreira R A S, Correia S F H, Monguzzi A, Liu X G and Meinardi F 2020 *Mater Today* **33** 105
[120] Chen S F, Peng B, Lu F, Mei Y, Cheng F, Deng L L, Xiong Q H, Wang L H, Sun X W and Huang W 2014 *Adv. Opt. Mater.* **2** 442
[121] Liang L L, Liu Y M, Bu C H, Guo K M, Sun W W, Huang N, Peng T, Sebo B, Pan M M, Liu W, Guo S S and Zhao X Z 2013 *Adv. Mater.* **25** 2174
[122] Ding Y L, Qiao H Z, Yang T H, Yin N Q, Li P, Zhao Y and Zhang X D 2017 *Opt. Mater.* **73** 617
[123] Yao H H, Peng G Q, Li Z Z, Zhu G, Li W Q, Ci Z P, Lan W, Jia H, Dong B and Jin Z W 2022 *J. Energy Chem.* **65** 524
[124] Qiao Y, Li S H, Liu W H, Ran M Q, Lu H F and Yang Y P 2018 *Nanomater* **8** 43
[125] Chen W H, Luo Q, Zhang C X, Shi J H, Deng X H, Yue L Y, Wang Z B, Chen X H and Huang S M 2017 *J. Mater. Sci.: Mater. Electron.* **28** 11346
[126] Rahman N U, Khan W U, Khan S, Chen X J, Khan J, Zhao J, Yang Z Y, Wu M M and Chi Z G 2019 *J. Mater. Chem. A* **7** 6467
[127] Jiang L, Chen W C, Zheng J W, Zhu L Z, Mo L, Li Z Q, Hu L H, Hayat T, Alsaedi A, Zhang C N and Dai S Y 2017 *ACS Appl. Mater. Interfaces* **9** 26958
[128] Jiang L, Zheng J W, Chen W C, Huang Y, Hu L H, Hayat T, Alsaedi A, Zhang C G and Dai S Y 2017 *ACS Appl. Energy Mater.* **1** 93
[129] Meng R Q, Feng X X, Yang Y W, Lv X D, Cao J and Tang Y 2019 *ACS Appl. Mater. Interfaces* **11** 13273
[130] Zhang B X, Song Z L, Jin J J, Bi W B, Li H, Chen C, Dai Q L, Xu L and Song H W 2019 *J. Colloid Interface Sci.* **553** 14
[131] Zheng H Y, Liu G Z, Zhu L Z, Ye J J, Zhang X H, Alsaedi A, Hayat T, Pan X and Dai S Y 2017 *ACS Appl. Mater. Interfaces* **9** 41006
[132] Bi W B, Wu Y J, Zhang B X, Jin J J, Li H, Liu L, Xu L, Dai Q L, Chen C and Song H W 2019 *ACS Appl. Mater. Interfaces* **11** 11481
[133] Hafez H,Wu J H, Lan Z, Li Q H, Xie G X, Lin J M, Huang M L and Huang Y F 2010 *Nanotechnology* **21** 415201
[134] Chander N, Khan A, Chandrasekhar P S, Thouti E, Swami S K, Dutta V and Komarala V K 2014 *Appl. Phys. Lett.* **105** 033904
[135] Jia J B, Dong J, Lin J M, Lan Z, Fan L Q and Wu J H 2019 *J. Mater. Chem. C* **7** 937
[136] Song P, Zhu P F and Zhang C M 2018 *J. Alloys Compd.* **731** 1009
[137] Li H, Chen C, Jin J J, Bi W B, Zhang B X, Chen X, Xu L, Liu D L, Dai Q L and Song H W 2018 *Nano Energy* **50** 699
[138] Zheng J F. Deng X S, Zhou X, Yu M D, Xia Z T, Chen X H and Huang S M 2019 *J. Mater. Sci.: Mater. Electron.* **30** 11043
[139] Liang L L, Liu Y M and Zhao X Z 2013 *Chem. Commun.* **49** 3958
[140] Wang Z, Quan Z and Lin J 2007 *Inorg. Chem.* **46** 5237
[141] Moon B, Kim S J, Lee S, Lee A, Lee H, Lee D S, Kim T W, Lee S K, Bae S and Lee S H 2019 *Adv. Mater.* **31** 1901716
[142] Alam F, Wegner K D, Pouget S, Amidani L, Kvashnina K, Aldakov D and Reiss P 2019 *J. Chem. Phys.* **151** 231101
[143] Huang J M, Lei T, Siron M, Zhang Y, Yu S, Seeler F, Dehestani A, Quan L N, Schierle Arndt K and Yang P D 2020 *Nano Lett.* **20** 3734
[144] Mitzi D B and Liang K N 1997 *Chem. Mater.* **9** 2990